Hydrodynamische Modelle und numerische Verfahren zur Beschreibung von Niedertemperaturplasmen

Markus Becker
D. Loffhagen

19.12.2011

Leibniz-Institut für Plasmaforschung und Technologie e.V.

Outline

Introduction

- Plasma science at the INP Greifswald

Surfaces & Materials

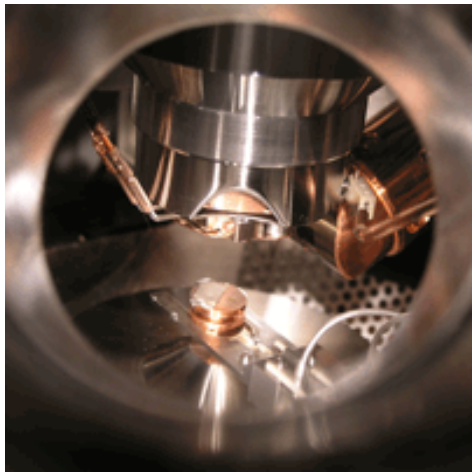

Environment & Energy

Biology & Medicine

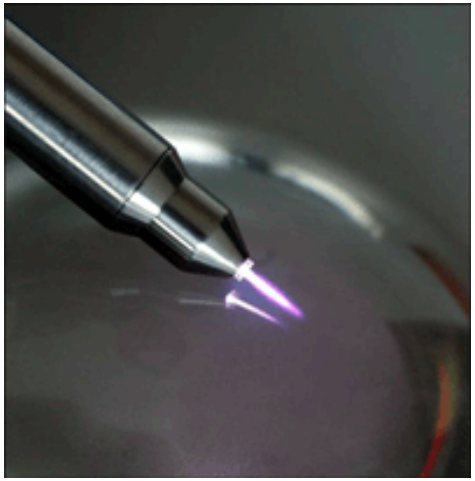

- Plasma modelling group contributes to all sectors
  - (better) understanding of fundamental processes
  - parameter studies and optimization
  - assistance for development of new devices

Basic features of modelling

Device / experimental setup

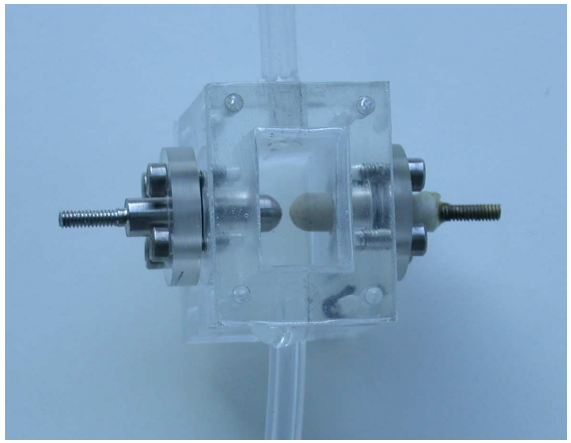

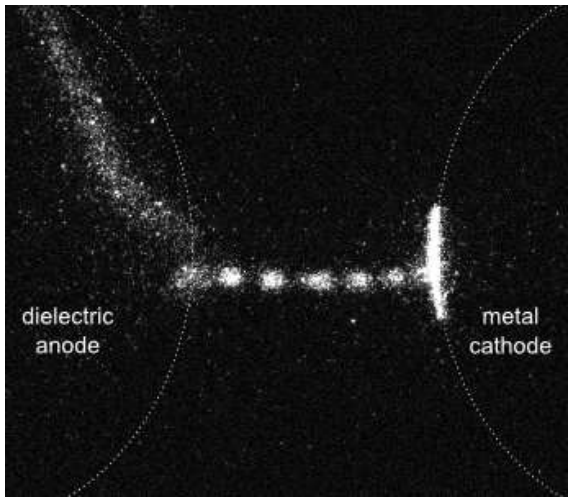

Basic features of modelling

Device / experimental setup

Mathematical model

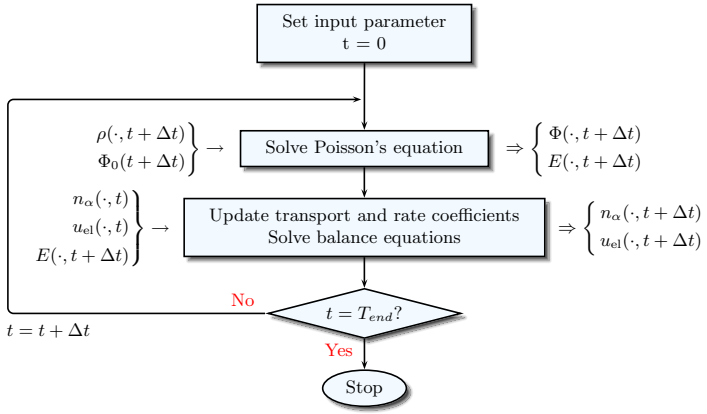

Basic features of modelling

Device / experimental setup

Mathematical model

Computer program

```
REAL(kind=rp) :: F_m,F_p,V_p,x_m,x_p
REAL(kind=rp) :: g1,g2,g3,g4
REAL(kind=rp) :: h_m,h_p,h_c,dtdh

M = size(X)
allocate(Unew(M),S(M))
Unew = 0._rp
S = S_lhs*U+S_rhs
select case(order)
   case(1) ! simple upwind scheme
      i = 1
      h_p = X(i+1)-X(i)
      V_p = 0.5_rp*(V(i)+V(i+1))
      F_p = max(0._rp,V_p)*U(i)+min(0._rp,V_p)*U(i+1)
      do i=2,M-1
         h_m = h_p
```

Basic features of modelling

Device / experimental setup

Mathematical model

Computer program

Prediction of plasma behaviour

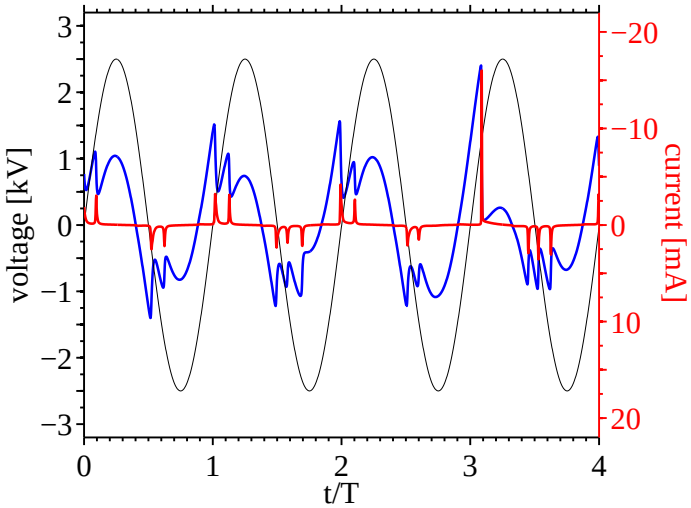

Possible approaches for plasma modelling

- Kinetic model
  - PIC-MCC / direct solution of a kinetic equation
  - most accurate but very time-consuming
- Hydrodynamic model
  - Solution of a certain set of fluid equations
  - most efficient but less accurate
- Hybrid (kinetic $\leftrightarrow$ hydrodynamic) model
  - kinetic model for (fast) electrons, fluid model for heavy particles

Fields of application

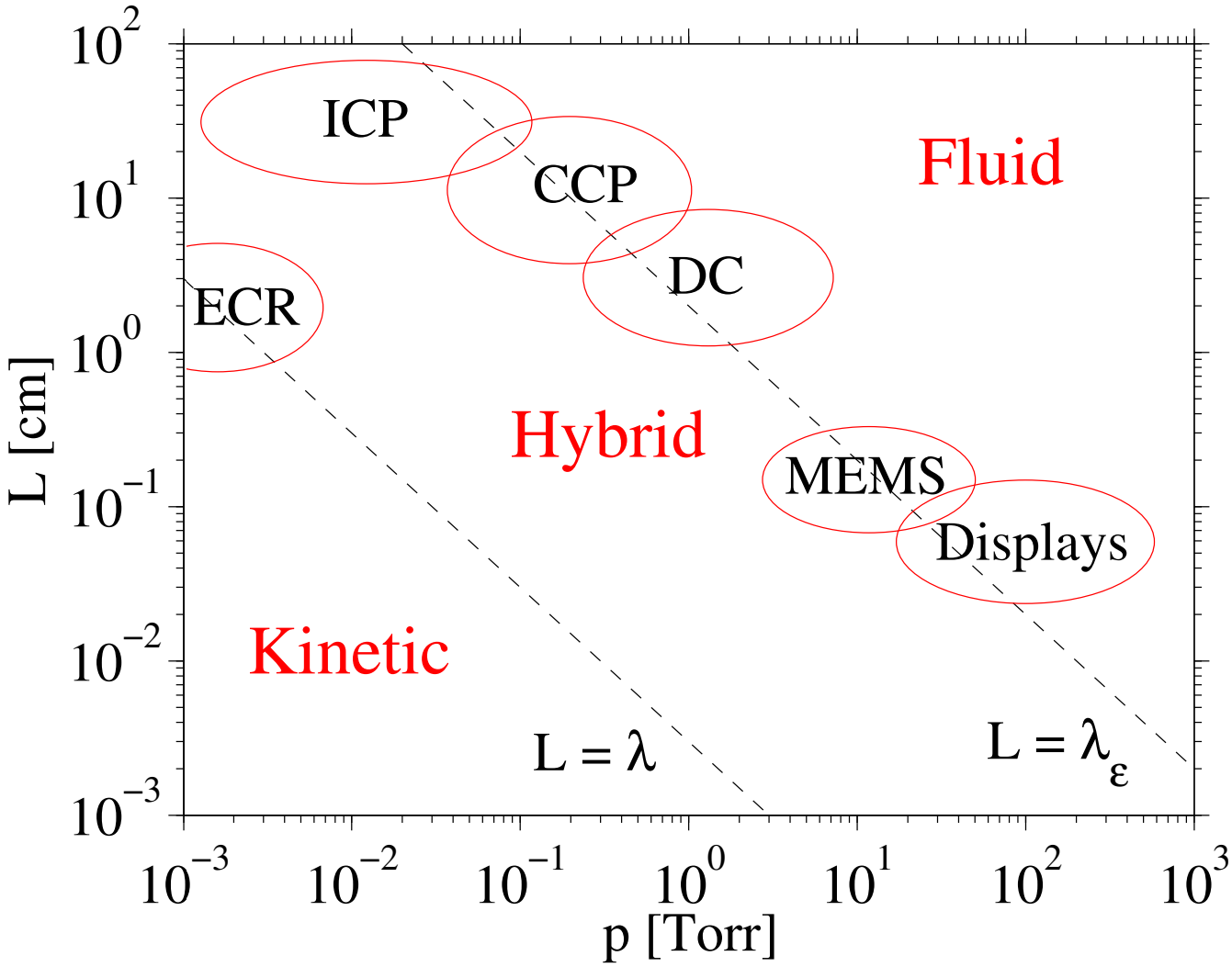

Derivation of fluid equations

Boltzmann equation for the velocity distribution function

$$\partial_t f_s + \boldsymbol{v} \cdot \nabla f_s + \frac{q_s}{m_s} \boldsymbol{E} \cdot \nabla_v f_s = \sum_h \left(C_h^{\mathrm{el}}(f_s) + \sum_r C_{h,r}^{\mathrm{in}}(f_s) \right)$$

Direct derivation

Strict hydrodynamic models

Balance equations for
- particle density
- particle flux
- energy density
- + assumption for heat flux

Further simplifications

Drift-diffusion model

Derivation of fluid equations

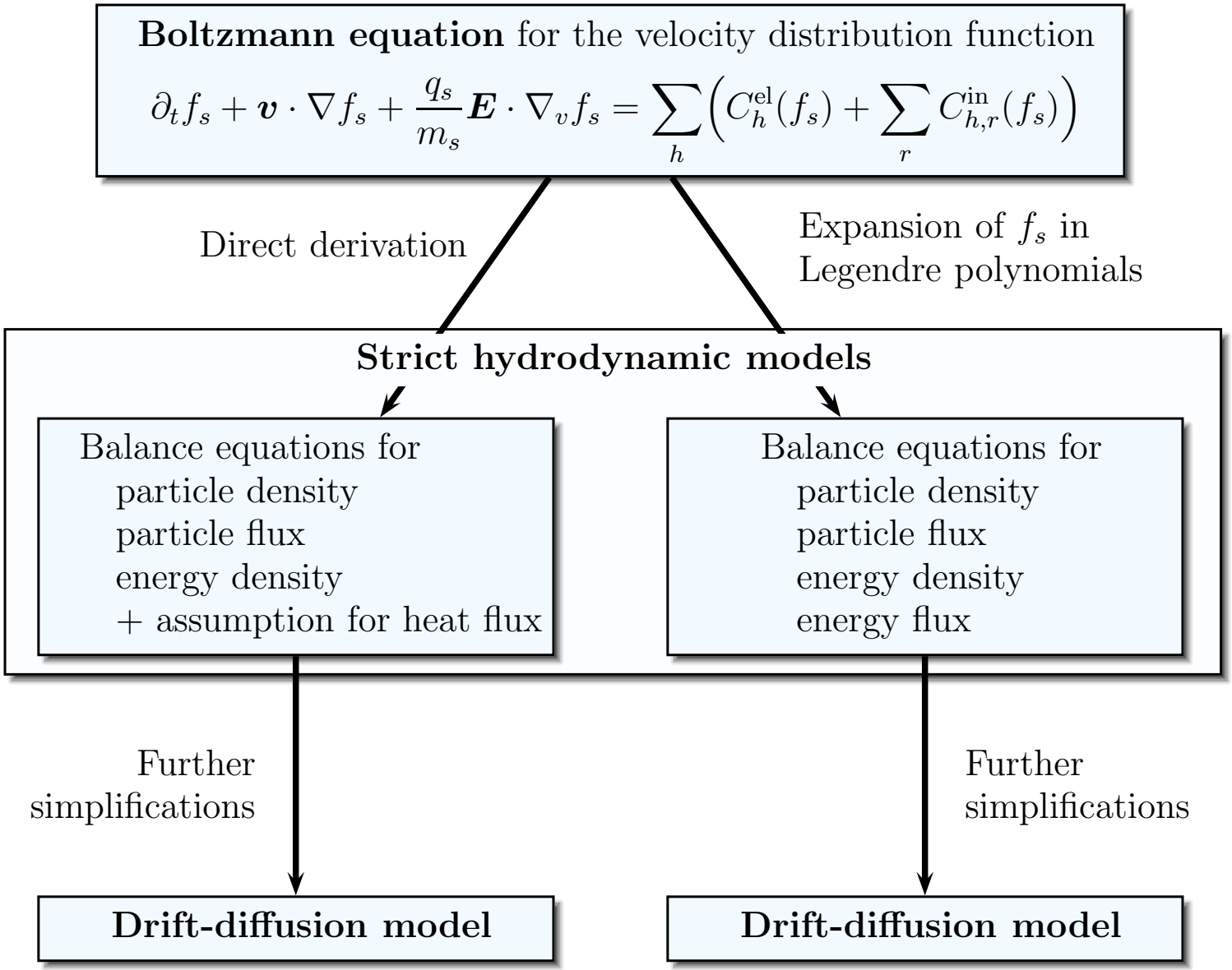

Derivation of fluid equations

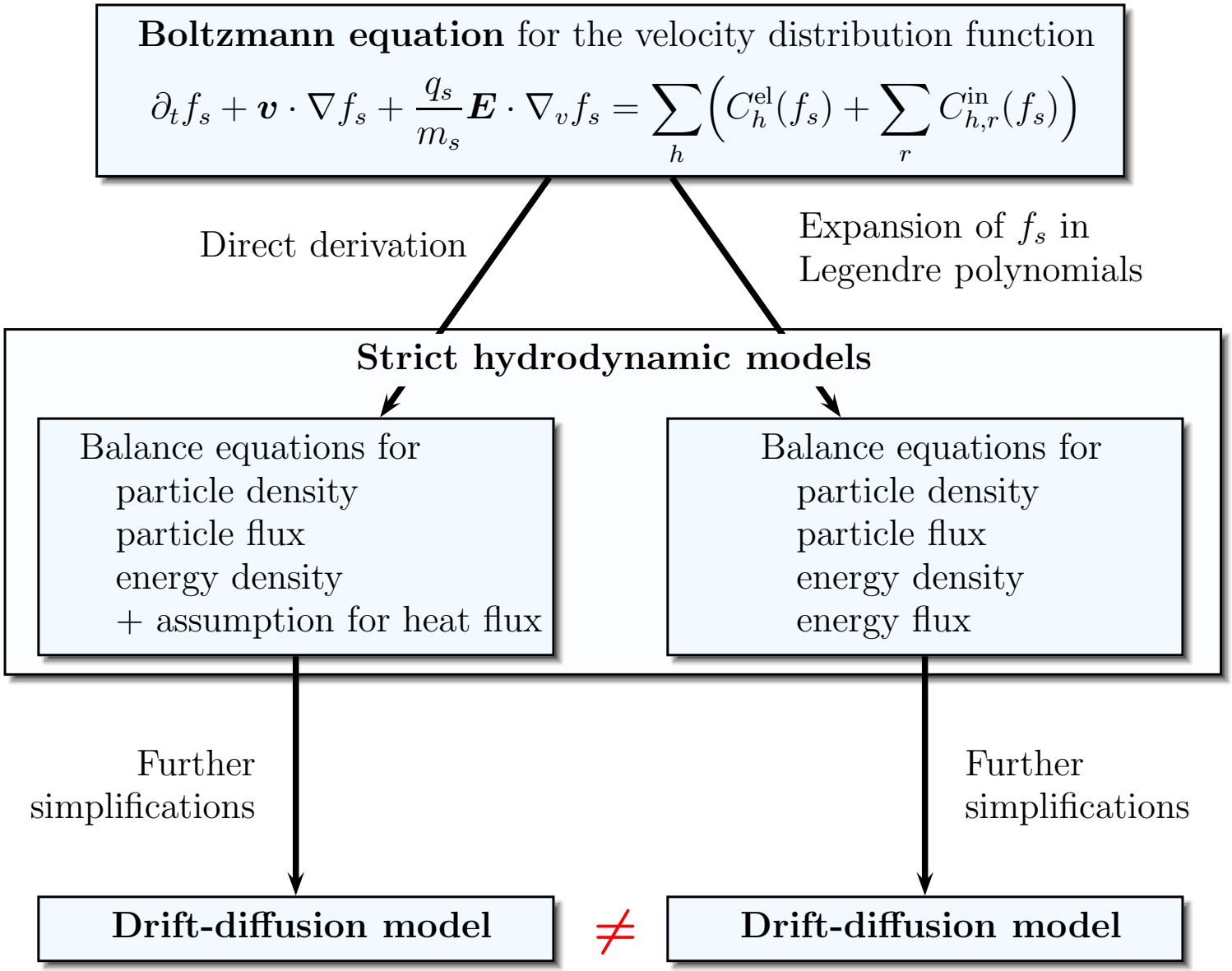

Strict hydrodynamic model

- Multiplying Boltzmann's equation by 1, $\boldsymbol{v}$ and $\frac{1}{2}m_s v^2$
  $\Rightarrow$ governing equations for n_s, $\boldsymbol{\Gamma}_s = n_s \bar{\boldsymbol{v}}_s$ and w_s

$$\partial_t n_s + \nabla \cdot \boldsymbol{\Gamma}_s = S_s$$

$$\partial_t \boldsymbol{\Gamma}_s + \nabla \cdot \left(\bar{\boldsymbol{v}}_s \otimes \boldsymbol{\Gamma}_s\right) + \nabla\left(\frac{2}{3}\frac{w_s}{m_s} - \frac{1}{3}\boldsymbol{\Gamma}_s \cdot \bar{\boldsymbol{v}}_s\right) = \frac{q_s}{m_s} n_s \boldsymbol{E} - \nu_s \boldsymbol{\Gamma}_s$$

$$\partial_t w_s + \nabla \cdot \left(\frac{5}{3} w_s \bar{\boldsymbol{v}}_s - \frac{m_s}{3}\boldsymbol{\Gamma}_s \cdot \bar{\boldsymbol{v}}_s \bar{\boldsymbol{v}}_s + \mathbf{q}_s\right) = q_s \boldsymbol{E} \cdot \boldsymbol{\Gamma}_s + \tilde{S}_s$$

- Poisson's equation for the electric potential

$$-\varepsilon_0 \Delta \Phi = \sum_s q_s n_s; \qquad \boldsymbol{E} = -\nabla \Phi$$

Common assumptions

- Fourier's law for heat flux of electrons

$$\mathbf{q}_\mathrm{e} = -\kappa_\mathrm{e} \nabla(\bar{\varepsilon}) \quad \text{with} \quad \bar{\varepsilon} = \frac{w_\mathrm{e}}{n_\mathrm{e}} \approx \frac{3}{2} k_\mathrm{B} T_\mathrm{e}$$

  $\Rightarrow$ parabolic-hyperbolic system for n_e, $\boldsymbol{\Gamma}_\mathrm{e}$ and w_e

- Temperature of heavy particles assumed to be constant (energy balance equation not needed)
  $\Rightarrow$ hyperbolic system for n_h and $\boldsymbol{\Gamma}_\mathrm{h}$

- Resulting system of partial differential equations has the general form

$$\partial_t \boldsymbol{U} + \nabla \cdot \boldsymbol{F}(\boldsymbol{U}) = \boldsymbol{R}(\boldsymbol{U})$$

Drift-diffusion model

- Continuity equations for the particle densities

$$\partial_t n_s + \nabla \cdot \boldsymbol{\Gamma}_s = S_s$$

- Energy balance equation for electrons

$$\partial_t w_\mathrm{e} + \nabla \cdot \boldsymbol{Q}_\mathrm{e} = \tilde{S}_\mathrm{e}$$

- Drift-diffusion approximation for particle and energy fluxes

$$\boldsymbol{\Gamma}_s = -\nabla(D_s n_s) + \mathrm{sgn}(q_s) b_s \boldsymbol{E}\, n_s$$
$$\boldsymbol{Q}_\mathrm{e} = -\nabla(\tilde{D}_\mathrm{e} n_\mathrm{e}) - \tilde{b}_\mathrm{e} \boldsymbol{E}\, n_\mathrm{e}$$

- Poisson's equation for the electric potential

$$-\varepsilon_0 \Delta \Phi = \sum_s q_s n_s; \qquad \boldsymbol{E} = -\nabla \Phi$$

Electron transport coefficients

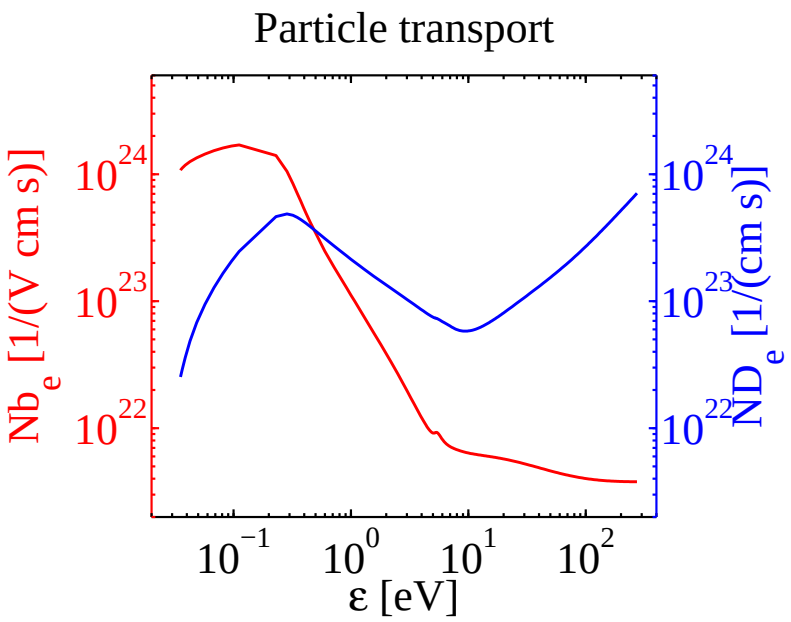

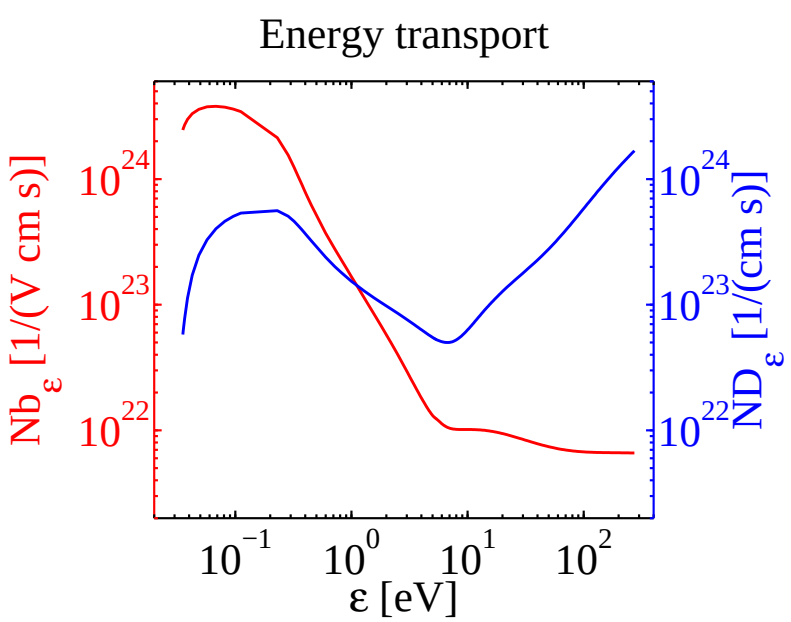

- Electron transport coefficients as functions of the mean energy obtained from solution of 0D Boltzmann equation

Ion transport coefficients

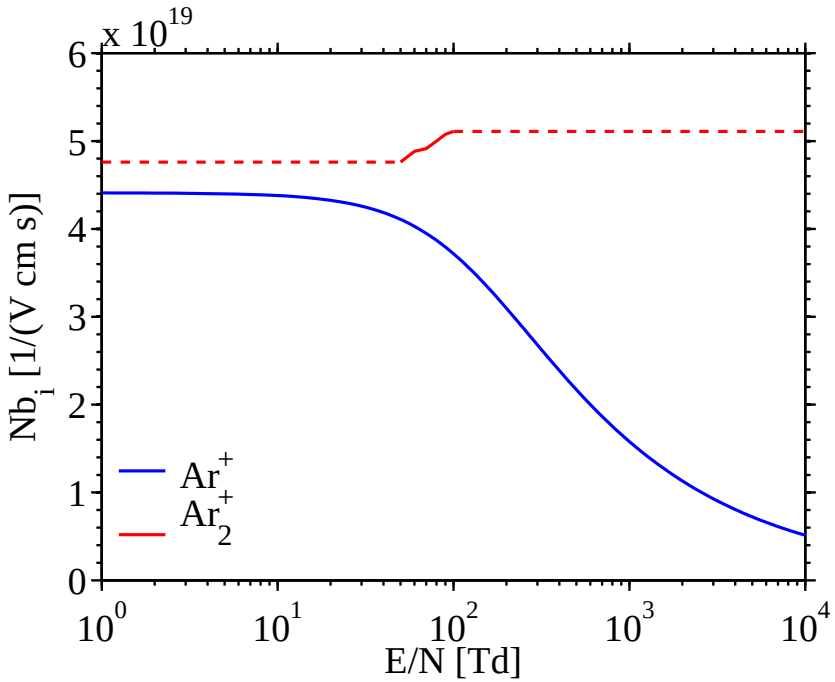

A. V. Phelps, J. Phys. Chem. Ref. Data **20**, 557 (1991)
H.W. Ellis *et al.*, At. Data and Nucl. Data Tables **31**, 113 (1984)

- Ion transport coefficients are taken from literature
- Ion mobility b_i depends on E/N
- Einstein relation for determination of diffusion coefficient

Source terms

- Gain and loss of particles and energy due to
  - collisions: $A + B + \ldots \quad \longrightarrow \quad C + D + \ldots$
  - radiation: $A \quad \longrightarrow \quad B + h\nu$

- Particle gain and loss

$$S_s = \sum_{i \in \mathcal{R}_s^{\mathrm{g}}} k_i g_{s,i} \prod_{k=1}^{N_s} n_k^{\beta_{k,i}} - \sum_{i \in \mathcal{R}_s^{\mathrm{l}}} k_i g_{s,i} \prod_{k=1}^{N_s} n_k^{\beta_{k,i}}$$

- Energy gain and loss

$$\tilde{S}_s = \sum_{i \in \mathcal{R}_s^{\mathrm{g}}} h_i k_i \prod_{k=1}^{N_s} n_k^{\beta_{k,i}} - \sum_{i \in \mathcal{R}_s^{\mathrm{l}}} h_i k_i \prod_{k=1}^{N_s} n_k^{\beta_{k,i}} - n_s P^{\mathrm{el}}$$

Boundary conditions

- Reflexion of heavy particles

$$\boldsymbol{\Gamma}_s \cdot \mathbf{n} = \frac{1 - r_s}{1 + r_s} \left(|b_s \boldsymbol{E} \cdot \mathbf{n}| \, n_s + \frac{v_{\mathrm{th,s}}}{2} \, n_s \right)$$

- Reflexion and secondary emission of electrons

$$\boldsymbol{\Gamma}_{\mathrm{e}} \cdot \mathbf{n} = \frac{1 - r_{\mathrm{e}}}{1 + r_{\mathrm{e}}} \left(|b_{\mathrm{e}} \boldsymbol{E} \cdot \mathbf{n}| \, n_{\mathrm{e}} + \frac{v_{\mathrm{th,e}}}{2} \, n_{\mathrm{e}}^{\alpha} \right) - \frac{2}{1 + r_{\mathrm{e}}} \gamma [\![\boldsymbol{\Gamma}_{\mathrm{i}}^{\mathrm{tot}} \cdot \mathbf{n}, 0]\!]$$

$$\boldsymbol{Q}_{\mathrm{e}} \cdot \mathbf{n} = \frac{1 - r_{\mathrm{e}}}{1 + r_{\mathrm{e}}} \left(|\tilde{b}_{\mathrm{e}} \boldsymbol{E} \cdot \mathbf{n}| \, n_{\mathrm{e}} + \frac{\tilde{v}_{\mathrm{th,e}}}{2} \, n_{\mathrm{e}}^{\alpha} \right) - \frac{2}{1 + r_{\mathrm{e}}} \bar{\varepsilon}^{\gamma} \gamma [\![\boldsymbol{\Gamma}_{\mathrm{i}}^{\mathrm{tot}} \cdot \mathbf{n}, 0]\!]$$

G.J.M. Hagelaar, F.J. de Hoog, G.M.W. Kroesen, Phys. Rev. E. **62**, 1452 (2000)

- Boundary conditions for the electric potential Φ

$$\Phi(0, t) = U_0 \big(1 - \exp(-t/\tau) \big); \qquad \Phi(d, t) = 0$$

Gas discharge model

- Spatially one-dimensional geometry

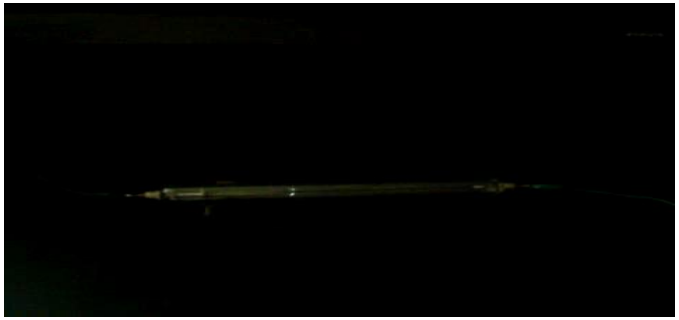

- Electrode gap $d = 1\,\mathrm{cm}$
- Gas: argon
- Gas pressure $p = 133\,\mathrm{Pa}$
- Gas temperature $T_\mathrm{g} = 300\,\mathrm{K}$
- Applied voltage $U_0 = -250\,\mathrm{V}$

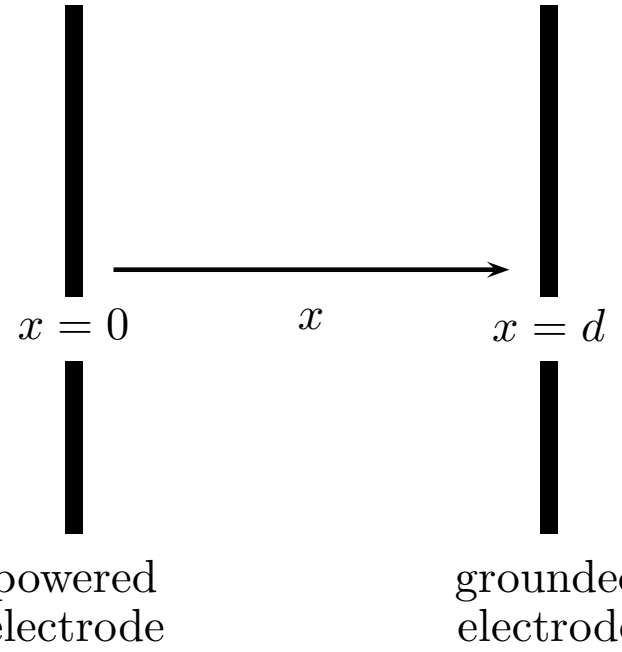

Ignition behaviour

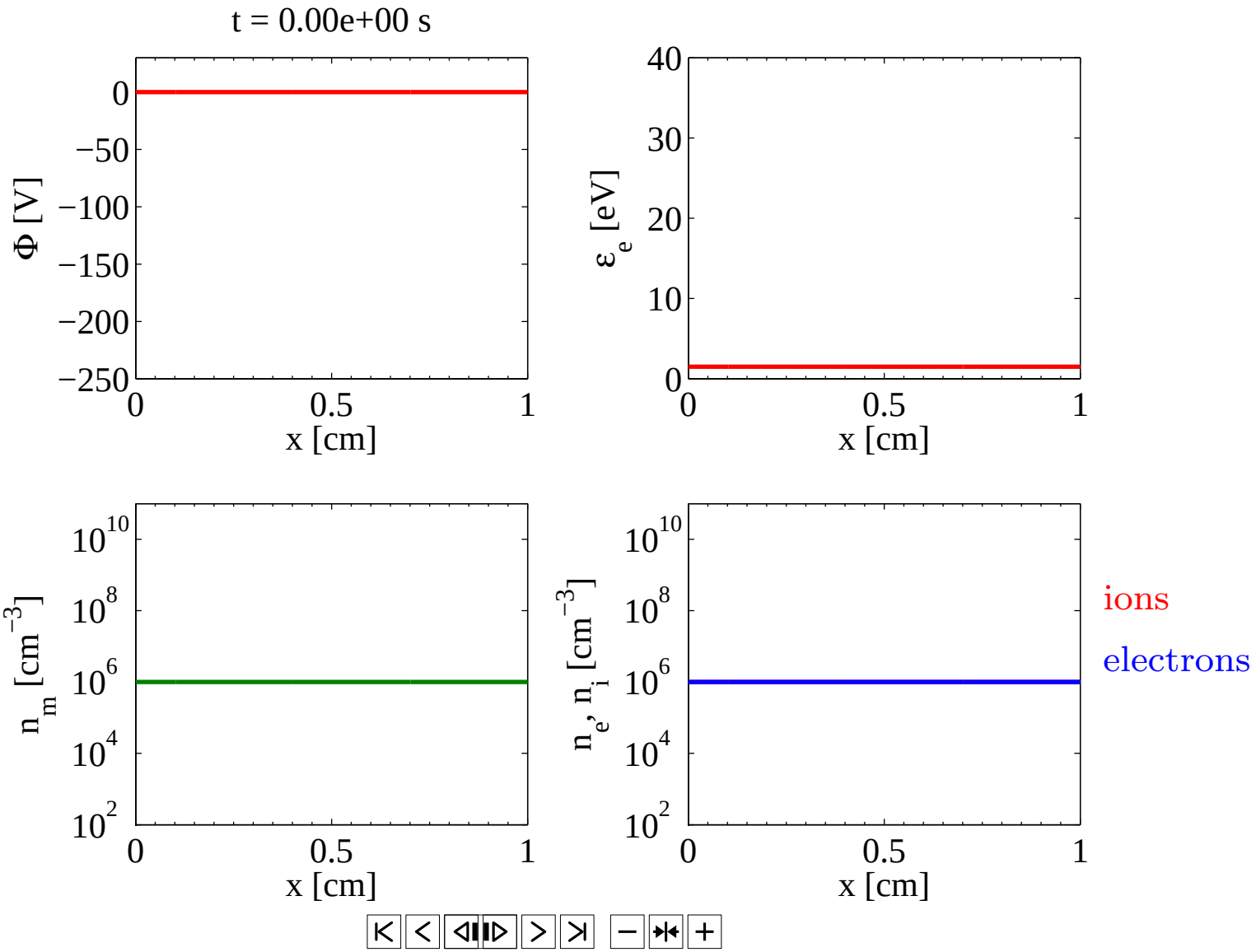

Numerical methods

- Numerical methods needed for discretization of the
  - strict hydrodynamic model including $\partial_t \boldsymbol{\Gamma}_s$
  - drift-diffusion model

- Special issues to deal with
  - parabolic/hyperbolic character changes in space and time
  - (locally) very fine spatial grids unavoidable
  - physical time scales strongly vary in time

Discretization techniques

- Standard FDM / Galerkin FEM for Poisson's equation
- Semi-implicit time-stepping scheme

Discretization techniques

- Standard FDM / Galerkin FEM for Poisson's equation
- Semi-implicit time-stepping scheme

- Drift-Diffusion model
  - Scharfetter-Gummel FDM / stabilized Petrov-Galerkin FEM for charged particles
  - standard FDM / Galerkin FEM for neutral particles

M.M. Becker, D. Loffhagen, W. Schmidt, Comput. Phys. Commun. **180**, 1230–1241 (2009)

Discretization techniques

- Standard FDM / Galerkin FEM for Poisson's equation
- Semi-implicit time-stepping scheme

- Drift-Diffusion model
  - Scharfetter-Gummel FDM / stabilized Petrov-Galerkin FEM for charged particles
  - standard FDM / Galerkin FEM for neutral particles

M.M. Becker, D. Loffhagen, W. Schmidt, Comput. Phys. Commun. **180**, 1230–1241 (2009)

- Strict hydrodynamic model
  - flux-corrected-transport methods based on FDM / FEM for balance equations

M.M. Becker, D. Loffhagen, Proc. Appl. Math. Mech. **10**, 641–642 (2010)

FEM for the drift-diffusion model

- For any $t \in]0, T_{\mathrm{end}}[$ find $\Phi(\cdot, t) \in V$ such that

$$\int_0^d \partial_x \Phi \, \partial_x v \, \mathrm{d}x = \frac{1}{\varepsilon_0} \int_0^d \sum_s q_s n_s \, v \, \mathrm{d}x \quad \forall \, v \in H_0^1((0,d))$$

- For any $t \in]0, T_{\mathrm{end}}[$ find $n_s(\cdot, t) \in V$, $s = 1, \ldots, N_s$ and $w_{\mathrm{e}}(\cdot, t) \in V$ such that

$$\partial_t \int_0^d n_s \, v \, \mathrm{d}x - \int_0^d \Gamma_s \, \partial_x v \, \mathrm{d}x = \int_0^d S_s \, v \, \mathrm{d}x + B_s \, v \Big|_0^d \quad \forall \, v \in H^1((0,d))$$

$$\partial_t \int_0^d w_{\mathrm{e}} \, v \, \mathrm{d}x - \int_0^d Q_{\mathrm{e}} \, \partial_x v \, \mathrm{d}x = \int_0^d \tilde{S}_{\mathrm{e}} \, v \, \mathrm{d}x + \tilde{B}_{\mathrm{e}} \, v \Big|_0^d \quad \forall \, v \in H^1((0,d))$$

Galerkin FEM

- Galerkin FEM: $S_h^s = T_h^s = \text{span}\{\varphi_0, \ldots, \varphi_{M_h}\}$

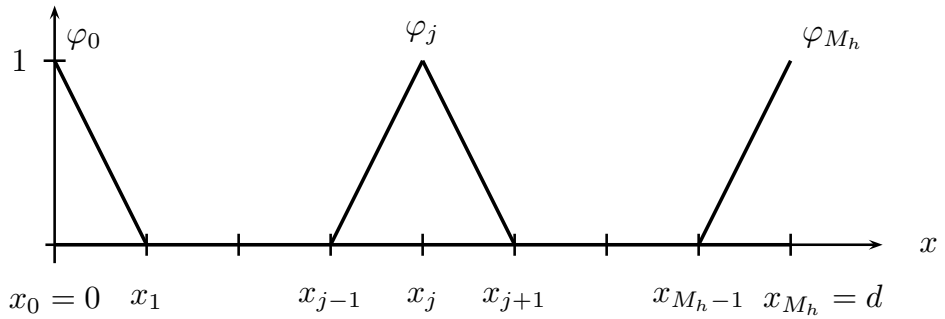

linear

- Optimal results for the potential and neutral particles

$$\|\tilde{u} - \tilde{u}_h\|_{L^2} \leq Ch^2$$

- Problem in charged particle equations

$$\|\tilde{u} - \tilde{u}_h\|_{L^2} \to \infty \quad \text{for} \quad |\mathrm{Pe}| = h\frac{|bE|}{2D} \to \infty$$

Galerkin FEM

- Galerkin FEM: $S_h^s = T_h^s = \text{span}\{\varphi_0, \ldots, \varphi_{M_h}\}$

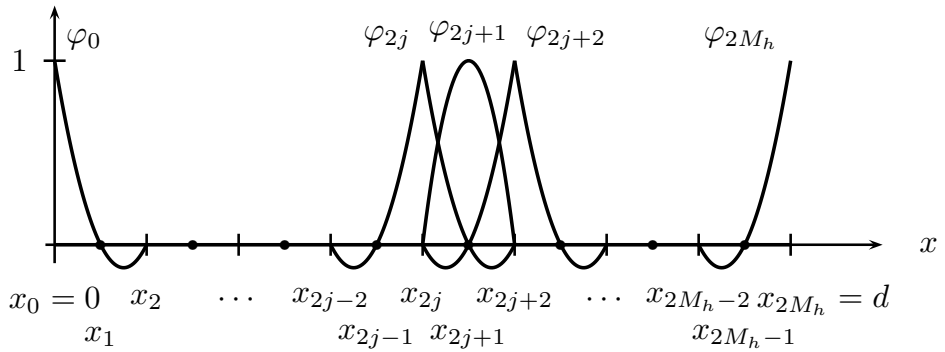

quadratic

- Optimal results for the potential and neutral particles

$$\|\tilde{u} - \tilde{u}_h\|_{L^2} \leq Ch^3$$

- Problem in charged particle equations

$$\|\tilde{u} - \tilde{u}_h\|_{L^2} \to \infty \quad \text{for} \quad |\text{Pe}| = h\frac{|bE|}{2D} \to \infty$$

Petrov-Galerkin FEM

- Stabilization by modifying the test space:
  $T_h^s = \text{span}\{\psi_0^s, \ldots, \psi_{M_h}^s\}$

$$\psi_j(x) = \begin{cases} \dfrac{x - x_{j-1}}{x_j - x_{j-1}} + \kappa \dfrac{3\,(x - x_{j-1})(x_j - x)}{(x_j - x_{j-1})^2} & , x_{j-1} \le x \le x_j \\ \dfrac{x_{j+1} - x}{x_{j+1} - x_j} - \kappa \dfrac{3\,(x - x_j)(x_{j+1} - x)}{(x_{j+1} - x)^2} & , x_j \le x \le x_{j+1} \\ 0 & , \text{otherwise} \end{cases}$$

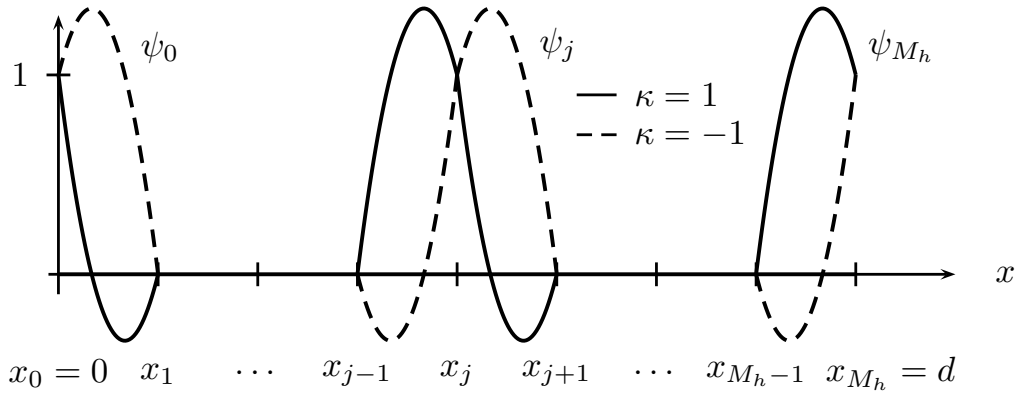

I. Christie *et al.*, Int. J. Numer. Meth. Eng. **10**, 1389 (1976)

Choice of the weighting factor

- Necessary condition for positivity

$$|\kappa| > \kappa_{\text{crit}} := 1 - \frac{1}{|\text{Pe}|}\,, \quad \text{sgn}(\kappa) = \text{sgn}(\text{Pe})$$

- Exact nodal values for stationary equations with constant coefficients

$$\kappa_{\text{opt}} := \coth(\text{Pe}) - \frac{1}{\text{Pe}}$$

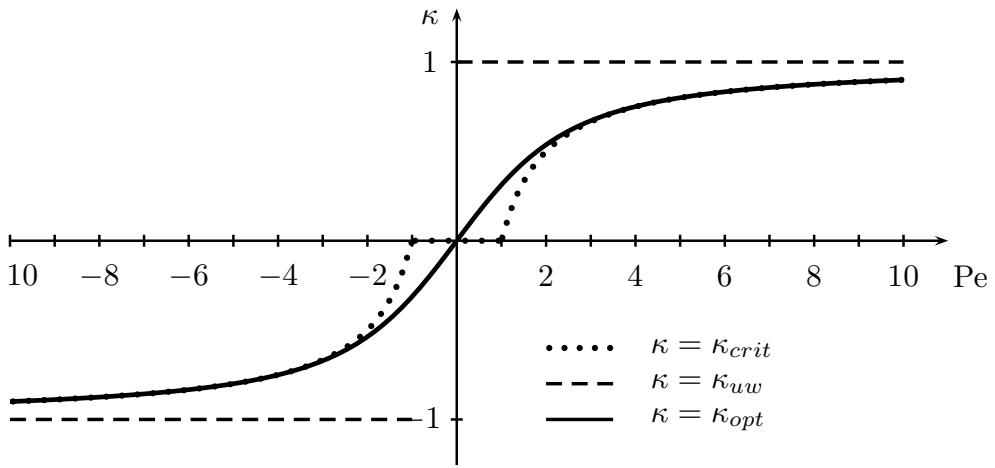

Comparison with FD and FV Methods

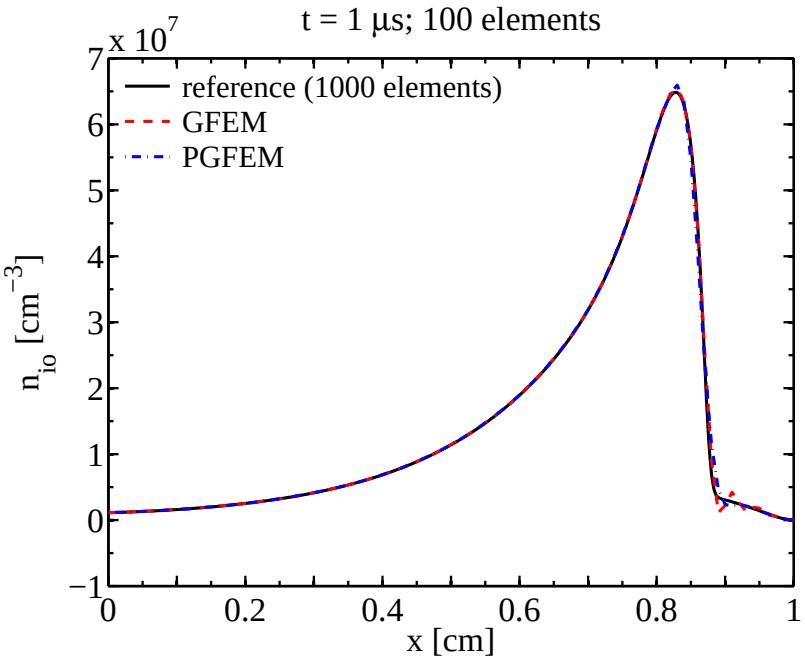

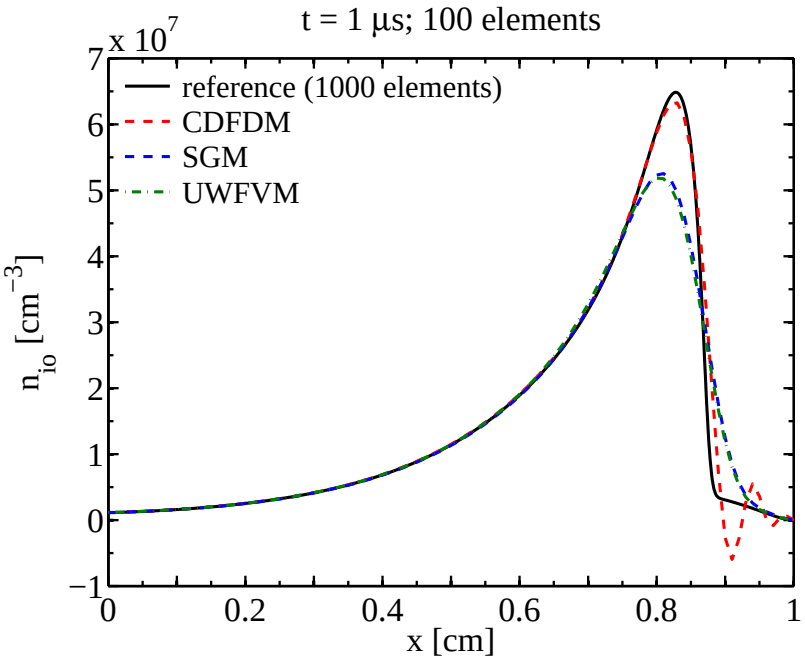

- PGFEM provides good results even on coarse spatial grids
- SGM and UWFVM yield non-oscillatory but inaccurate results on coarse spatial grids
- GFEM and CDFDM provide oscillating results if too coarse spatial grids are used

Comparison with FD and FV Methods

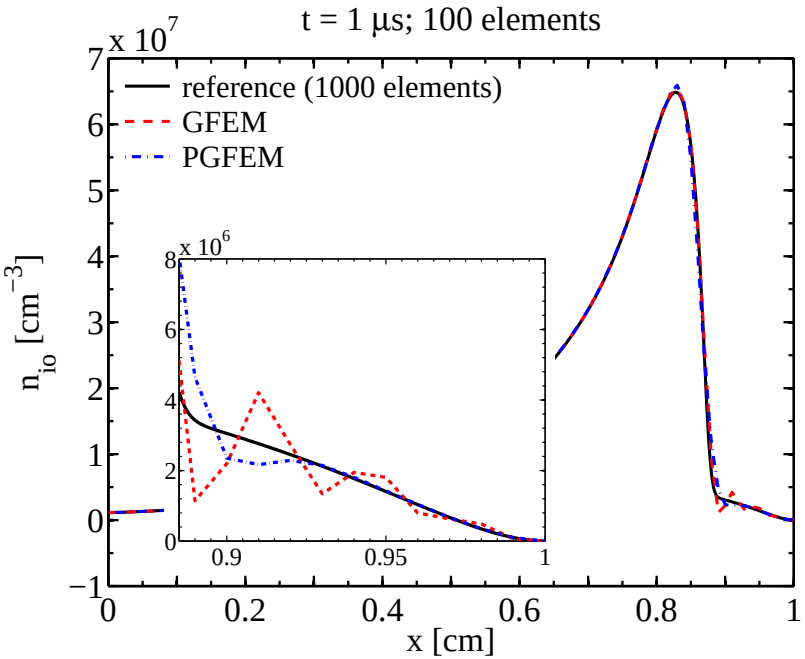

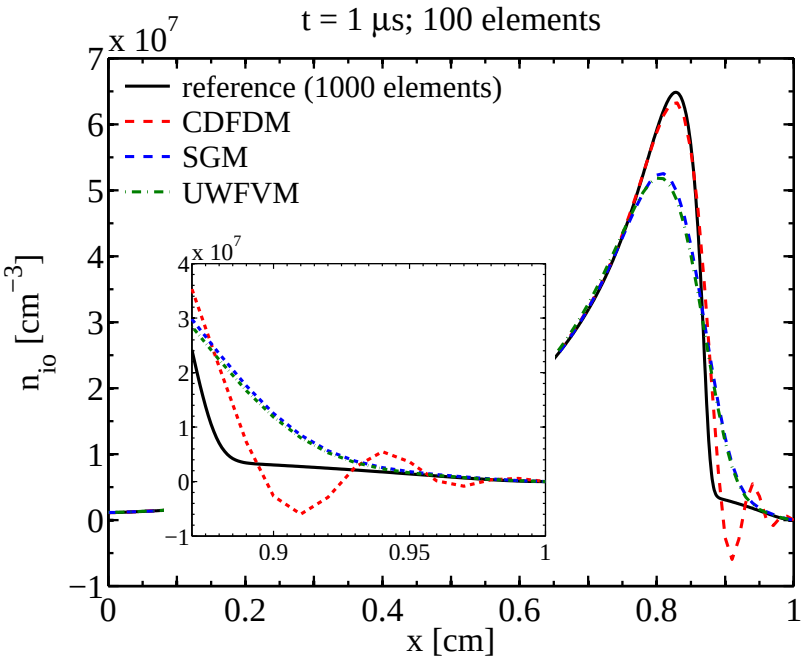

- PGFEM provides good results even on coarse spatial grids
- SGM and UWFVM yield non-oscillatory but inaccurate results on coarse spatial grids
- GFEM and CDFDM provide oscillating results if too coarse spatial grids are used

Comparison with FD and FV Methods

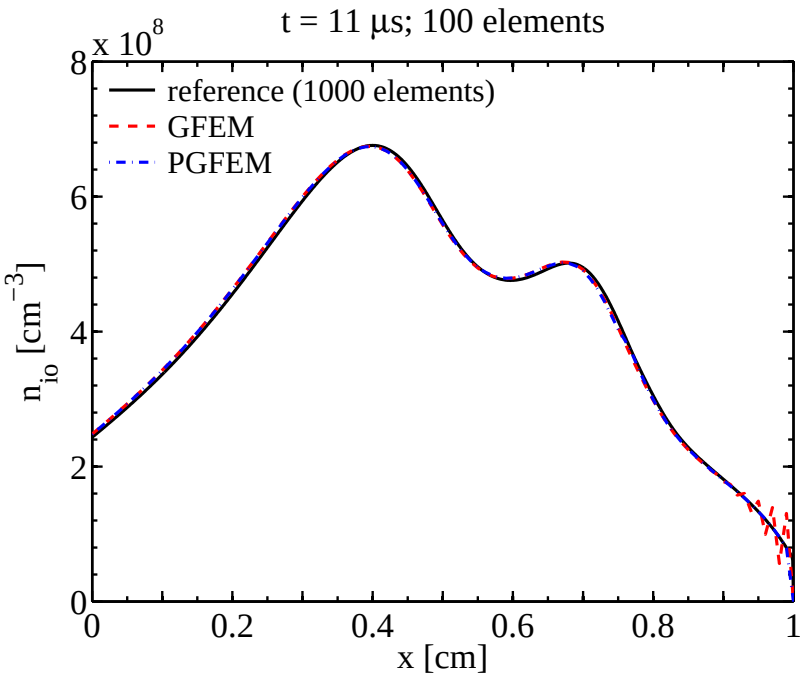

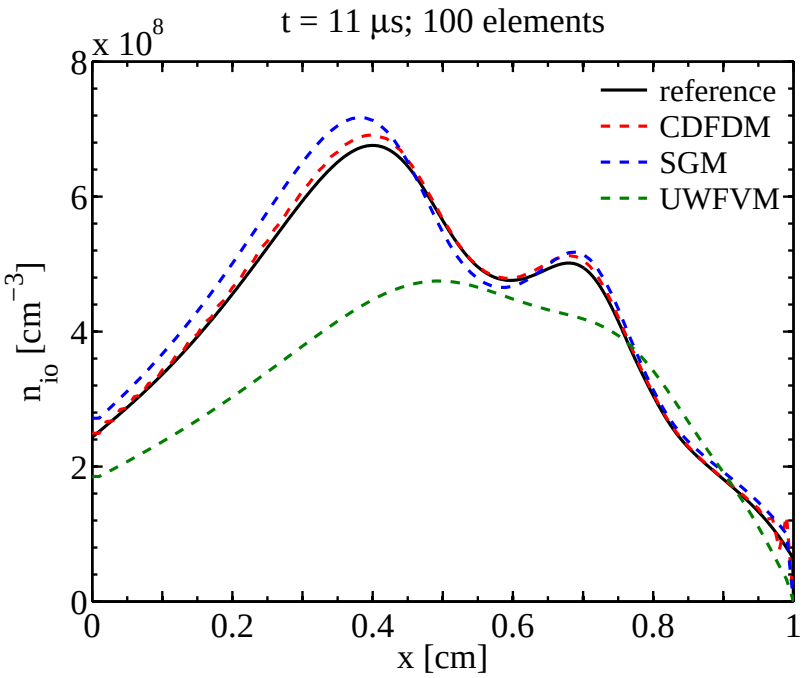

- Dirichlet outflow boundary condition
  $\Rightarrow$ oscillations when using GFEM or CDFDM and $|\mathrm{Pe}| > 1$
- Stabilized methods avoid this problem
- PGFEM provides better results than SGM and UWFVM

Comparison with FD and FV Methods

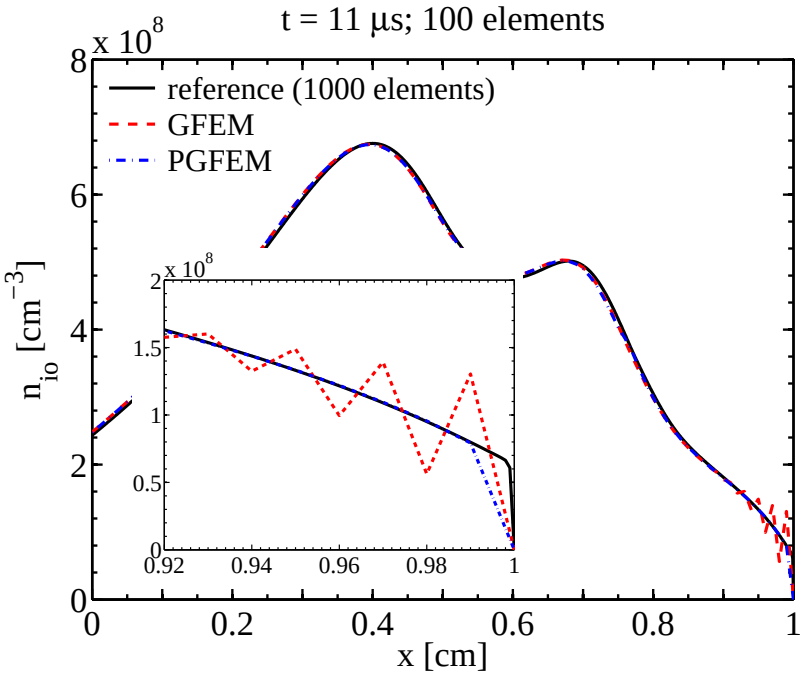

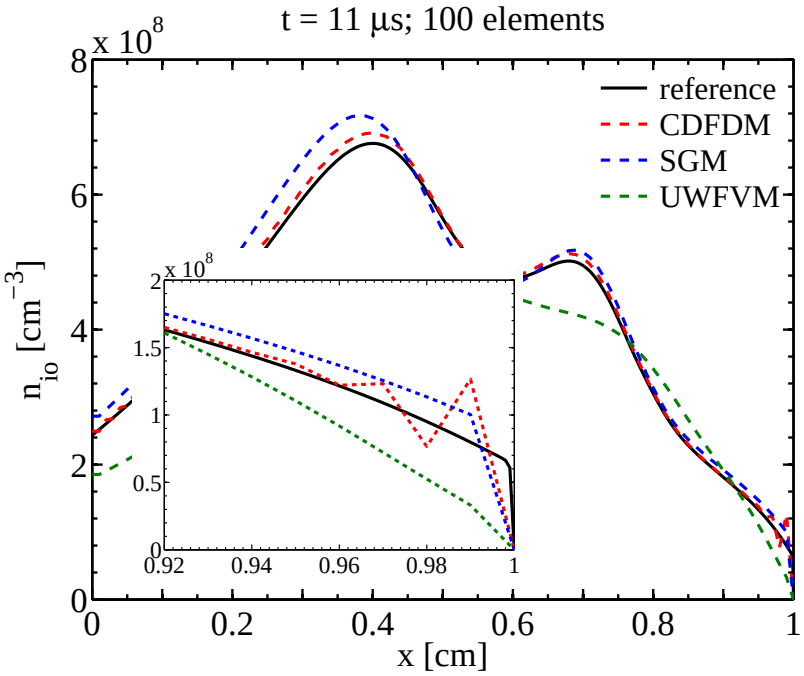

- Dirichlet outflow boundary condition
  $\Rightarrow$ oscillations when using GFEM or CDFDM and $|\mathrm{Pe}| > 1$
- Stabilized methods avoid this problem
- PGFEM provides better results than SGM and UWFVM

FCT for the strict hydrodynamic model

- Classical formulation for FDM

$$\partial_t U + \partial_x F = R$$

- Weak formulation for FEM

$$\int_0^d \partial_t U \, v \, \mathrm{d}x - \int_0^d F \partial_x v \, \mathrm{d}x = \int_0^d R \, v \, \mathrm{d}x \quad \forall \, v \in V$$

History of FCT

- 1973–1976 Boris/Book (ETBFCT)
- 1979 Zalesak
- 1984–1988 Erlbacher, Parrott/Christie, Löhner *et al.* (FEMFCT)
- 1993 Odstrcil (YDFCT)
- 2001–2009 Kuzmin *et al.* (FEMFCT)

ETBFCT (explicit) Boris/Book

1. Determination of high order (maybe oscillatory) solution

$$U_j^H = U_j^0 - \frac{\Delta t}{\Delta x}\left(F_{j+1/2}^0 - F_{j-1/2}^0\right) + \Delta t R_j^0$$

2. Determination of low order (monotonic) solution

$$U_j^L = U_j^H + \nu_{j+1/2}\Delta U_{j+1/2}^0 - \nu_{j-1/2}\Delta U_{j-1/2}^0$$

3. Determination of limited anti-diffusive fluxes

$$F_{j+1/2}^C = \mathrm{BBL}\left(U^L, \mu_{j+1/2}\Delta U_{j+1/2}^H\right)$$

4. Determination of final (corrected) solution

$$U_j^{\mathrm{new}} = U_j^L - \left(F_{j+1/2}^C - F_{j-1/2}^C\right)$$

$\rightarrow$ Time step restriction $\quad \mathrm{CFL} \leq 1/2$

- Diffusion and anti-diffusion coefficients reduce amplitude and phase errors to the fourth order (for pure convection on uniform grids)

$$\nu = \frac{1}{6} + \frac{1}{3}\left(\frac{v\Delta t}{\Delta x}\right)^2$$

$$\mu = \frac{1}{6} - \frac{1}{6}\left(\frac{v\Delta t}{\Delta x}\right)^2$$

- Boris/Book flux limiter

$$\mathrm{BBL}(U^L, F^A_{j+1/2}) = \mathrm{sgn}(\Delta U^L_{j+1/2}) \max\Big\{0, \min\big(|F^A_{j+1/2}|, \mathrm{sgn}(\Delta U^L_{j+1/2})\Delta U^L_{j-1/2}, \mathrm{sgn}(\Delta U^L_{j+1/2})\Delta U^L_{j+3/2}\big)\Big\}$$

ETBFCT (example)

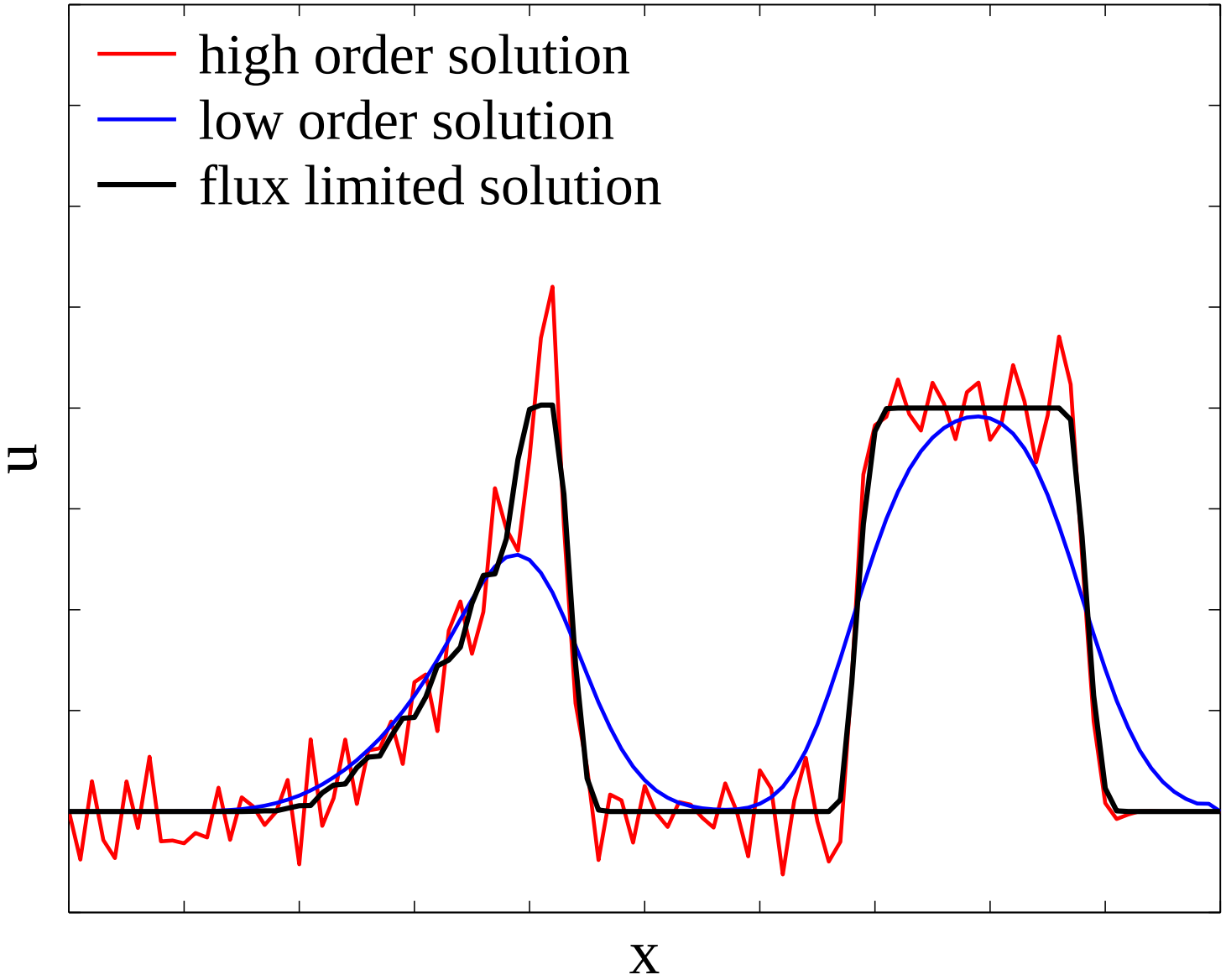

YDFCT (explicit) Odstrcil

Modifications with respect to ETBFCT:

- two steps per time step

$$U^0 \rightarrow U^* \rightarrow U^{\text{new}}$$

- additional diffusive fluxes in the first step

$$U_j^H = U_j^0 - \frac{\Delta t}{\Delta x}\left(F_{j+1/2}^0 - F_{j-1/2}^0\right) + \Delta t R_j^0 + \gamma_{j+1/2}\Delta U_{j+1/2}^0 - \gamma_{j-1/2}\Delta U_{j-1/2}^0$$

- modified anti-diffusive fluxes in the second step

$$F_{j+1/2}^C = \text{BBL}\left(U^L, \mu_{j+1/2}\max(|\Delta U_{j+1/2}^*|, \tfrac{1}{2}|\Delta U_{j+1/2}^H|\right)$$

$\rightarrow$ Time step restriction $\quad \text{CFL} \leq 1$

YDFCT (explicit) Odstrcil

- Additional anti-diffusion coefficient reduces the phase error to the sixth order (for pure convection on uniform grids)
- Half step:

$$\nu = \frac{1}{6} + \frac{1}{3}\left(\frac{v\Delta t}{2\Delta x}\right)^2 ; \quad \mu = \frac{1}{6} - \frac{1}{6}\left(\frac{v\Delta t}{2\Delta x}\right)^2$$

$$\gamma = \frac{1}{60} - \frac{1}{60}\left(\frac{v\Delta t}{2\Delta x}\right)^2$$

- Full step:

$$\nu = \frac{1}{3} + \frac{1}{6}\left(\frac{v\Delta t}{\Delta x}\right)^2 ; \quad \mu = \frac{1}{3} - \frac{1}{3}\left(\frac{v\Delta t}{\Delta x}\right)^2$$

FEMFCT (implicit) Kuzmin *et al.*

1. Determination of high order (maybe oscillatory) solution

$$\big(M - \Delta t K\big)\boldsymbol{U}^H = M\boldsymbol{U}^0 + \Delta t \boldsymbol{f}$$

2. Determination of anti-diffusive fluxes

$$\boldsymbol{F}^A = -\big((M - M_L) - \Delta t(K - K_D)\big)\boldsymbol{U}^H + (M - M_L)\boldsymbol{U}^0$$

3. Determination of limited anti-diffusive fluxes

$$\boldsymbol{F}^C = \mathrm{ZL}(\boldsymbol{F}^A, \boldsymbol{U}^0)\boldsymbol{F}^A$$

4. Determination of corrected (final) solution

$$\big(M_L - \Delta t K_D\big)\boldsymbol{U}^{\mathrm{new}} = M_L\boldsymbol{U}^0 + \Delta t \boldsymbol{f} + \boldsymbol{F}_C$$

FEMFCT (implicit) modified

1. Determination of high order (maybe oscillatory) solution

$$\big(M - \Delta t K_D\big)\boldsymbol{U}^H = M\boldsymbol{U}^0 + \Delta t \boldsymbol{f}$$

2. Determination of anti-diffusive fluxes

$$\boldsymbol{F}^A = -\big((M - M_L) - \Delta t(K - K_D)\big)\boldsymbol{U}^H + (M - M_L)\boldsymbol{U}^0$$

3. Determination of limited anti-diffusive fluxes

$$\boldsymbol{F}^C = \mathrm{ZL}(\boldsymbol{F}^A, \boldsymbol{U}^0)\boldsymbol{F}^A$$

4. Determination of corrected (final) solution

$$\big(M_L - \Delta t K_D\big)\boldsymbol{U}^{\mathrm{new}} = M_L\boldsymbol{U}^0 + \Delta t \boldsymbol{f} + \boldsymbol{F}_C$$

$\rightarrow$ Usage of K_D instead of K suppresses terracing effect

FEMFCT (implicit)

- FEMFCT uses adapted Zalesak limiter

$$P_i^{\pm} = \sum_{j \neq i} \mathop{\max}_{\min}\{0, F_{ij}^A\}$$

$$Q_i^{\pm} = \mathop{\max}_{\min} \Delta U_{ij}^{\pm}, \quad \text{where } \Delta U_{ij}^{\pm} = \mathop{\max}_{\min}\{0, U_j - U_i\}$$

$$R_i^{\pm} = \begin{cases} \min\{1, m_i Q_i^{\pm}/P_i^{\pm}\} & \text{if } P_i^{\pm} \neq 0 \\ 1, & \text{otherwise} \end{cases}$$

$$\alpha_{ij} = \begin{cases} \min\{R_i^+, R_j^-\} & \text{if } F_{ij}^A > 0 \\ \min\{R_j^+, R_i^-\} & \text{otherwise} \end{cases}$$

FEMFCT (example)

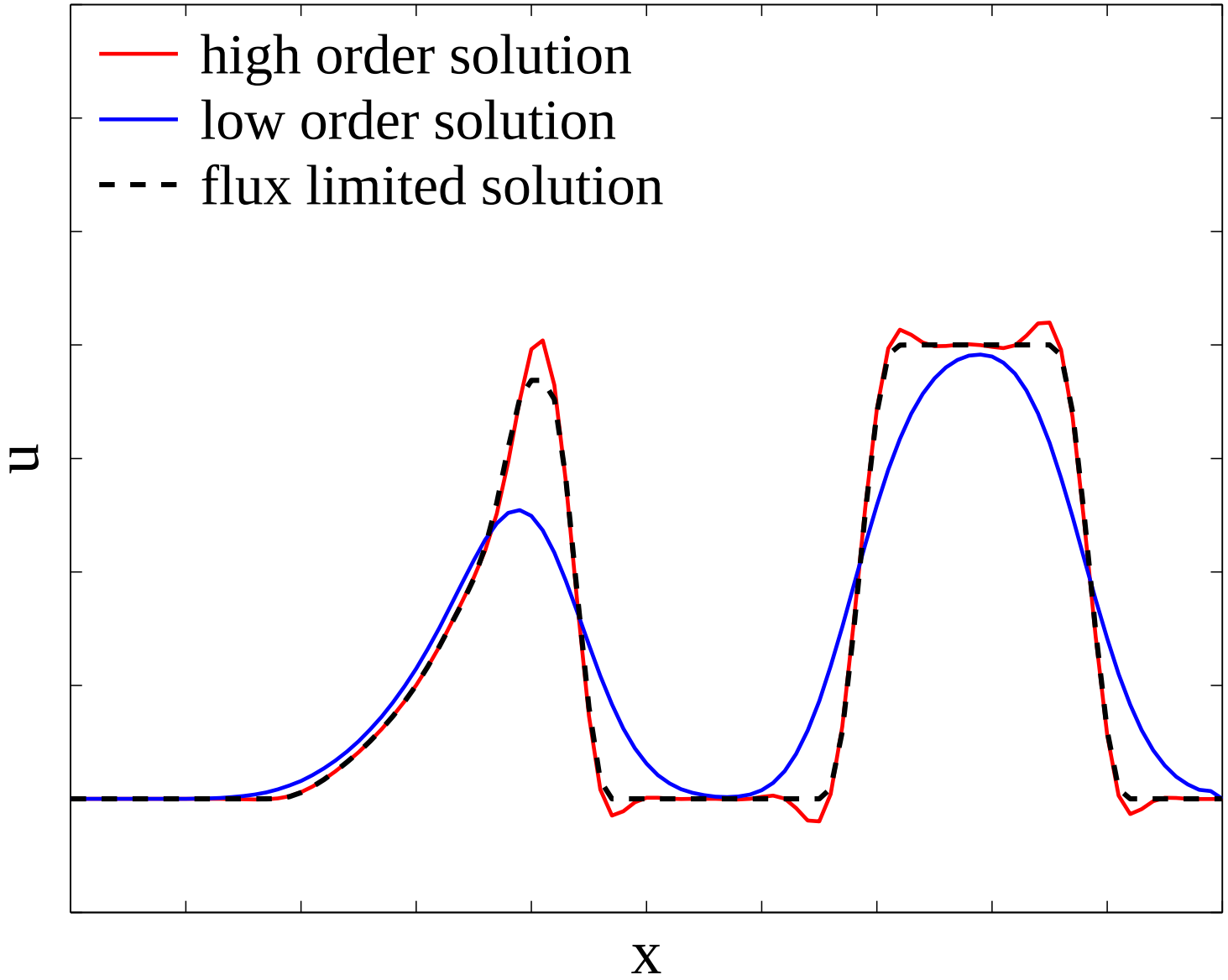

IFCT (implicit) new scheme

1. Determination of high order (maybe oscillatory) solution

$$U_j^H = U_j^0 - \frac{\Delta t}{\Delta x}\left(F_{j+1/2}^H - F_{j-1/2}^H\right) + \Delta t R_j^H + \gamma_{j+1/2}\Delta U_{j+1/2}^H - \gamma_{j-1/2}\Delta U_{j-1/2}^H$$

2. Determination of low order (monotonic) solution

$$U_j^L = U_j^0 - \frac{\Delta t}{\Delta x}\left(F_{j+1/2}^L - F_{j-1/2}^L\right) + \Delta t R_j^L + \nu_{j+1/2}\Delta U_{j+1/2}^L - \nu_{j-1/2}\Delta U_{j-1/2}^L$$

3. Determination of limited anti-diffusive fluxes

$$F_{j+1/2}^C = \mathrm{BBL}\left(U^L, \mu_{j+1/2}\Delta U_{j+1/2}^H\right)$$

4. Determination of final (corrected) solution

$$U_j^{\mathrm{new}} = U_j^L - \left(F_{j+1/2}^C - F_{j-1/2}^C\right)$$

Test case

- Pure convection with velocity $v = 1$

$$\partial_t \rho + \partial_x (v\rho) = 0$$

- Initial profile

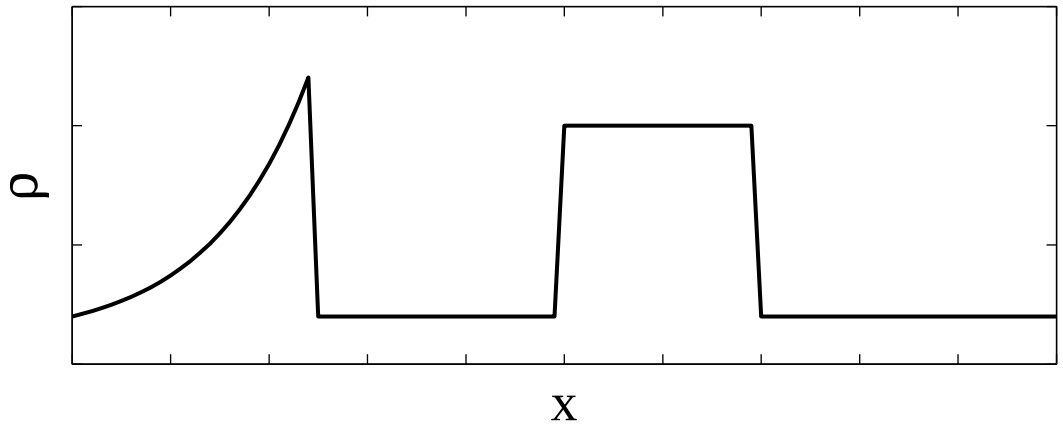

- 101 grid points, $\mathrm{CFL} = \dfrac{v\Delta t}{\Delta x} = 0.1$

Test case (explicit/implicit methods)

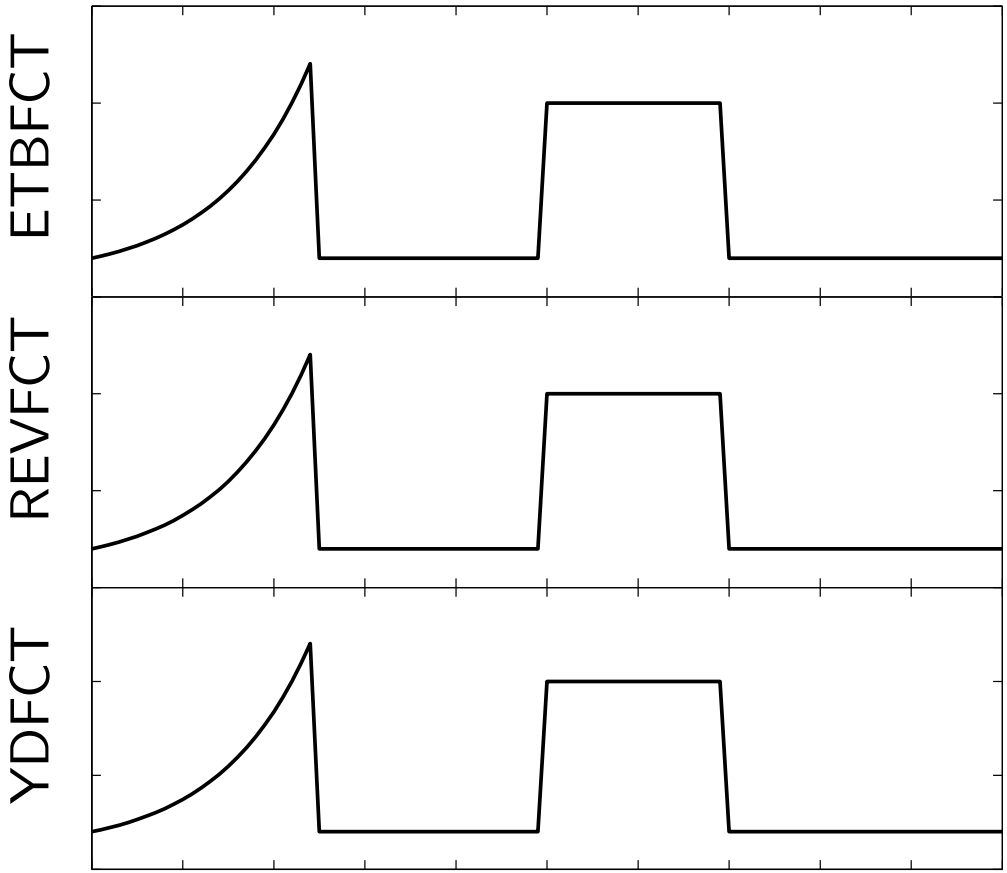

Test case (explicit/implicit methods)

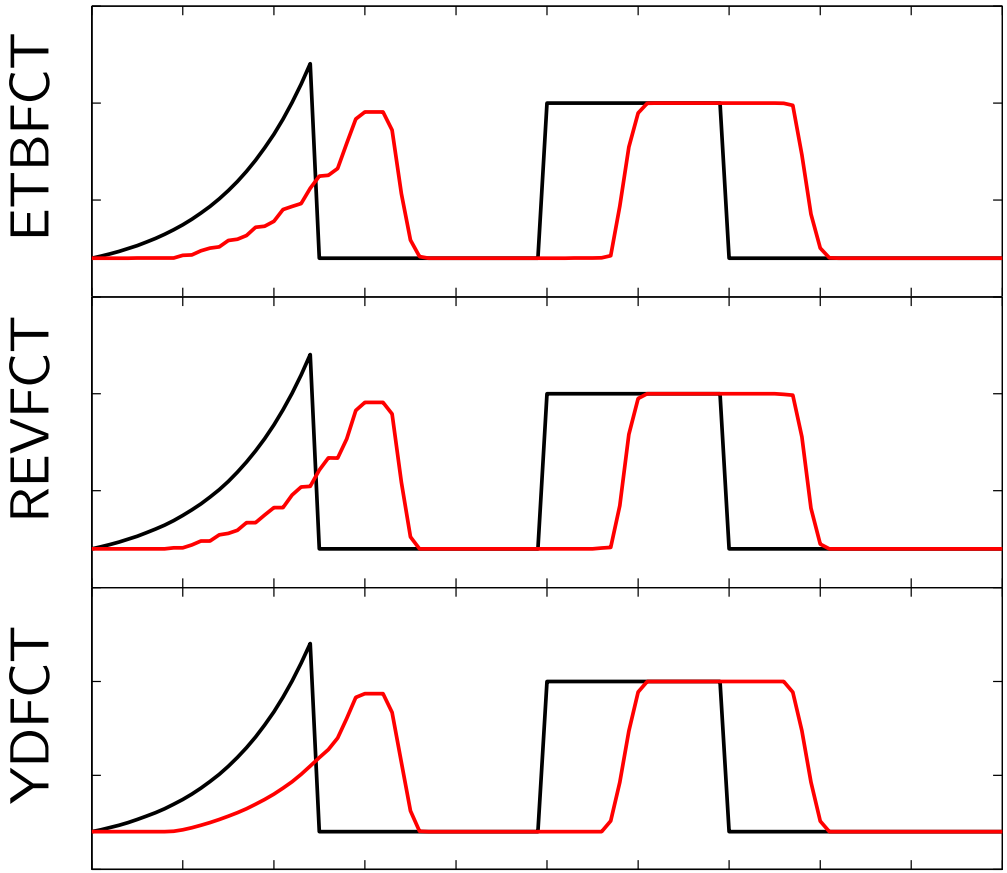

relative error: 0.066

relative error: 0.058

relative error: 0.069

after 90 time steps

- Adequate convection of the "square wave"
- ETBFCT and REVFCT exhibit terracing effect

Test case (explicit/implicit methods)

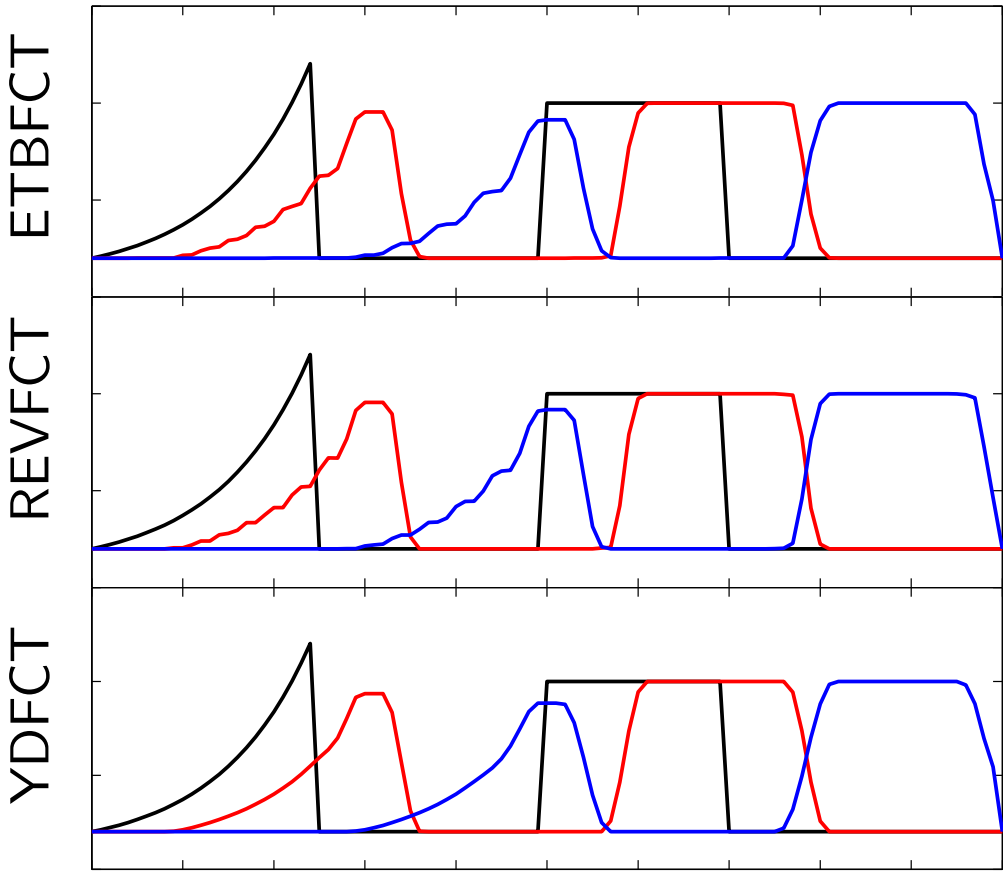

relative error: 0.066
relative error: 0.081

relative error: 0.058
relative error: 0.070

relative error: 0.069
relative error: 0.088

after 90 time steps
after 290 time steps

- Adequate convection of the “square wave”
- ETBFCT and REVFCT exhibit terracing effect

Test case (implicit methods)

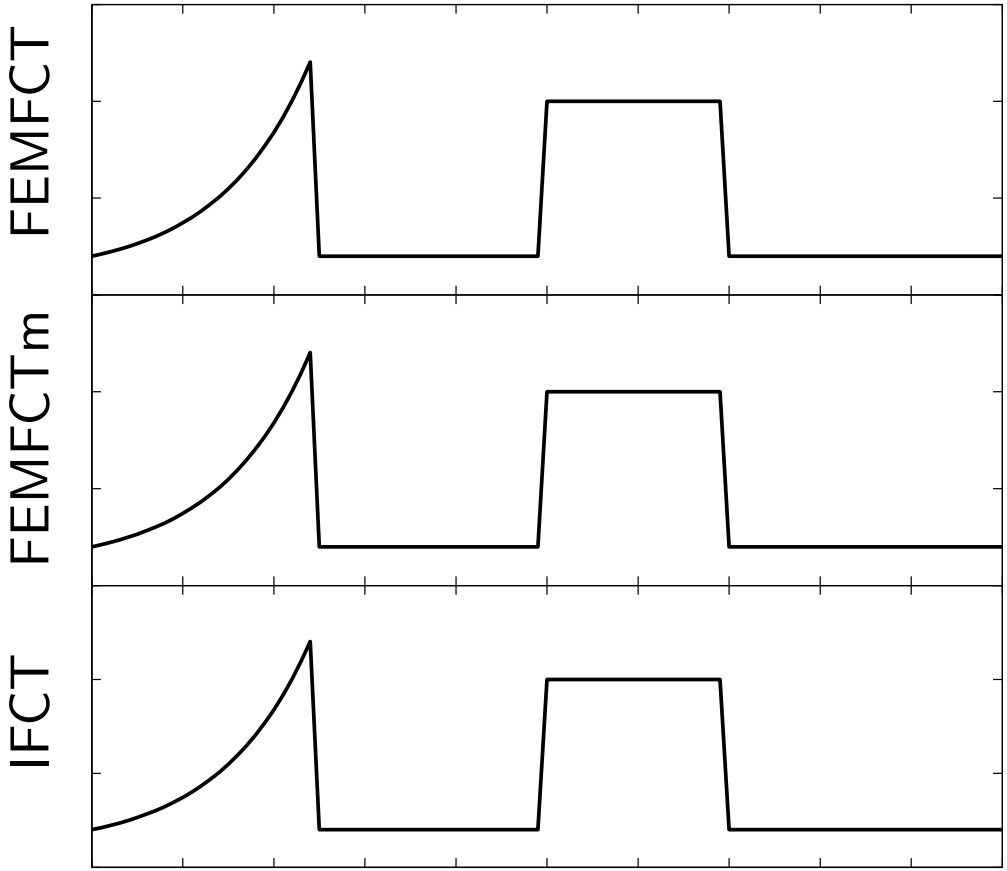

Test case (implicit methods)

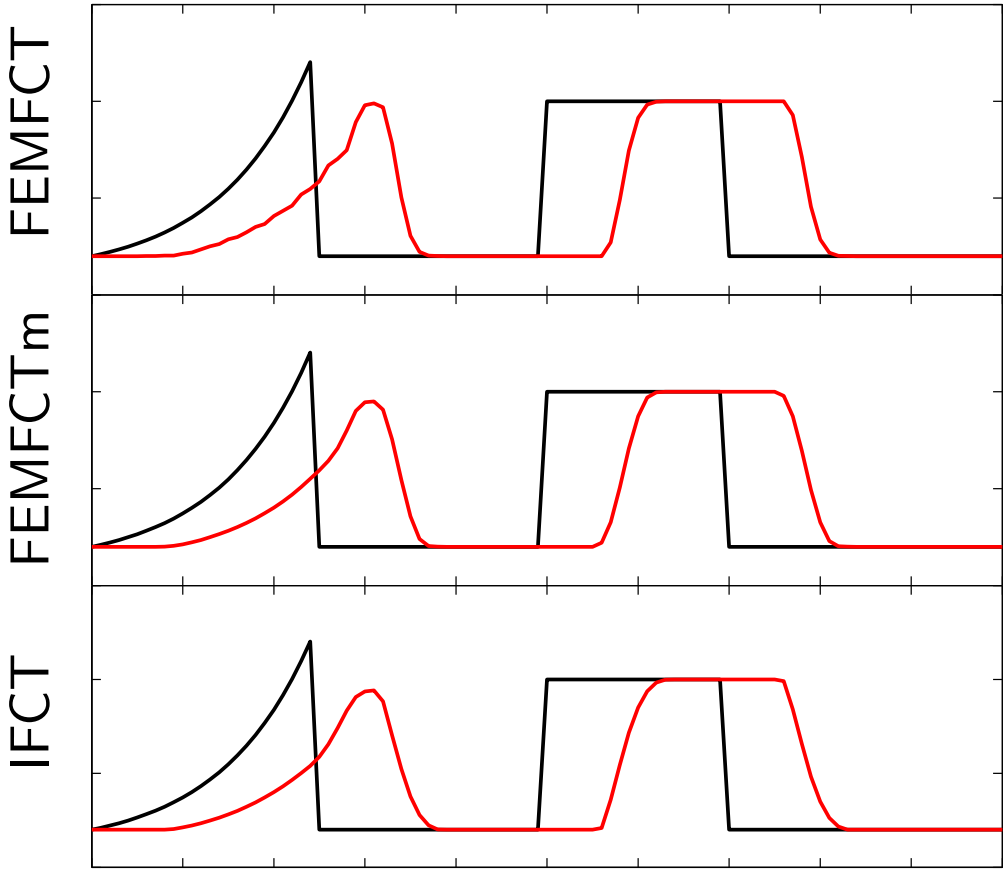

relative error: 0.073

relative error: 0.089

relative error: 0.101

after 90 time steps

- Terracing effect suppressed by modified FEMFCT and IFCT
- Implicit methods are more diffusive

Test case (implicit methods)

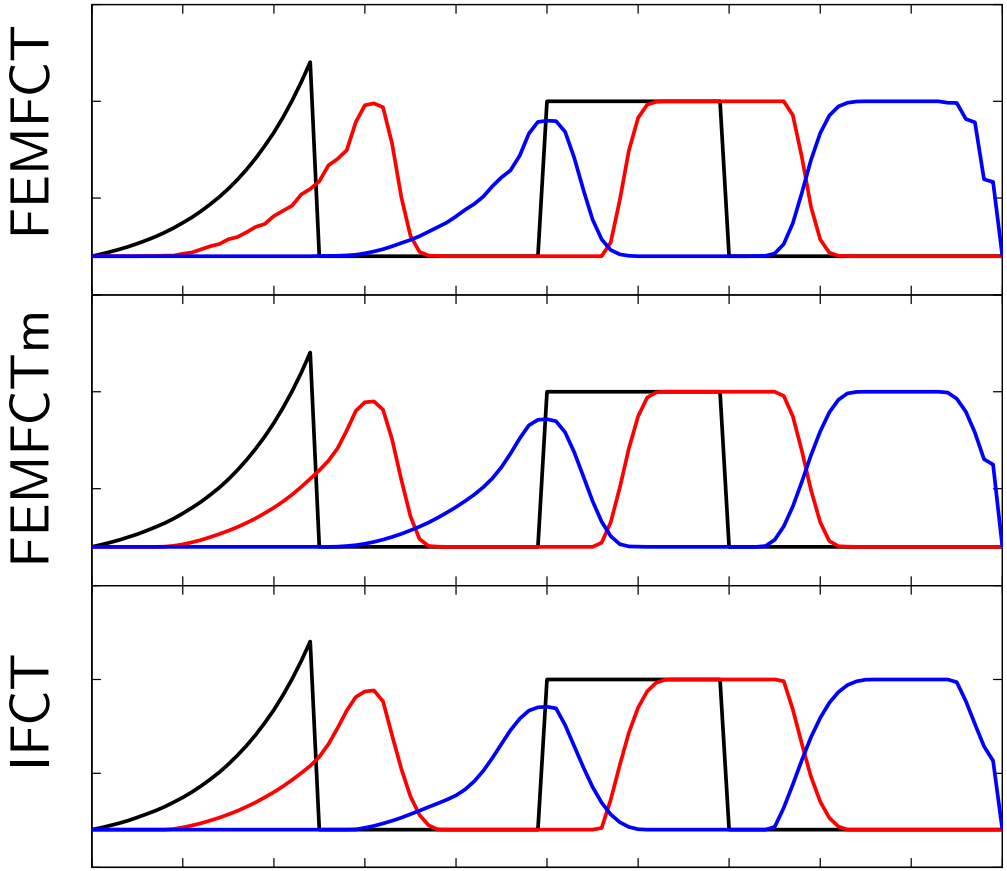

relative error: 0.073
relative error: 0.104

relative error: 0.089
relative error: 0.122

relative error: 0.101
relative error: 0.128

after 90 time steps
after 290 time steps

- Terracing effect suppressed by modified FEMFCT and IFCT
- Implicit methods are more diffusive

Gas discharge model

- Spatially one-dimensional geometry

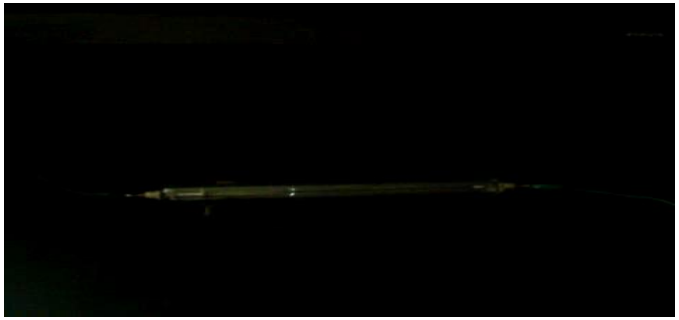

- Electrode gap $d = 1\,\mathrm{cm}$
- Gas: argon
- Gas pressure $p = 133\,\mathrm{Pa}$
- Gas temperature $T_\mathrm{g} = 300\,\mathrm{K}$
- Applied voltage $U_0 = -250\,\mathrm{V}$

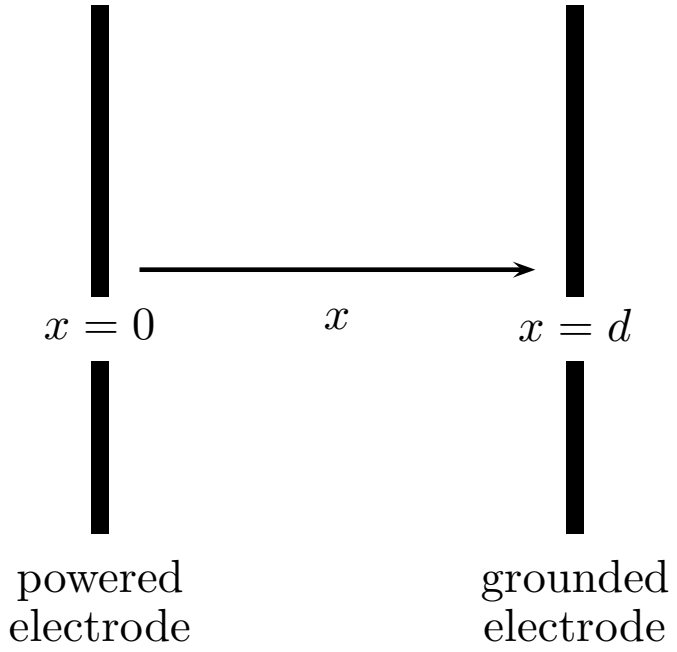

ETBFCT (201 grid points)

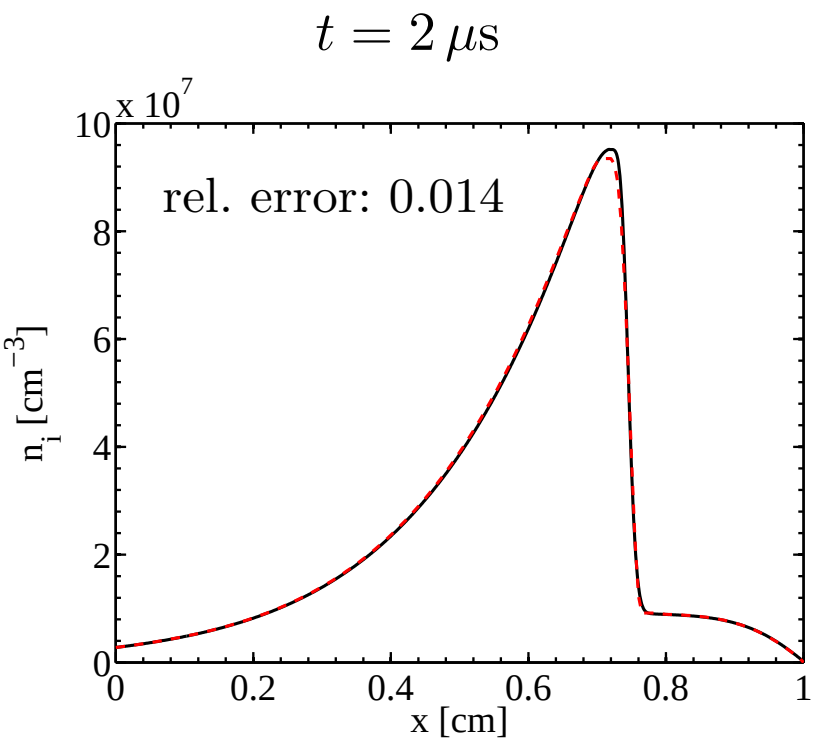

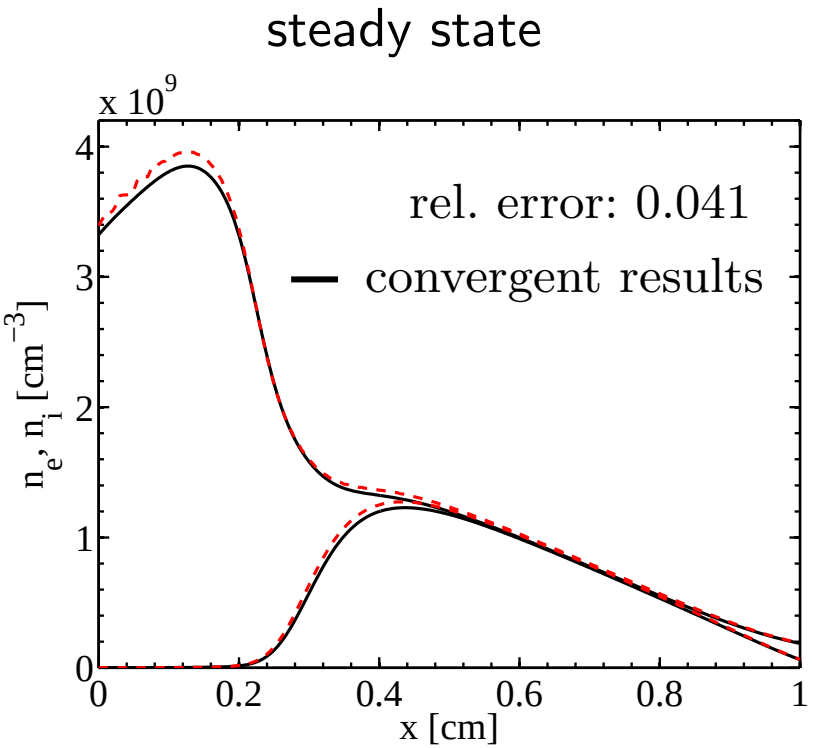

- Good approximation of steep gradients
- Spurious terracing effect
- (Locally) fine spatial grids not applicable due to CFL restriction

YDFCT (201 grid points)

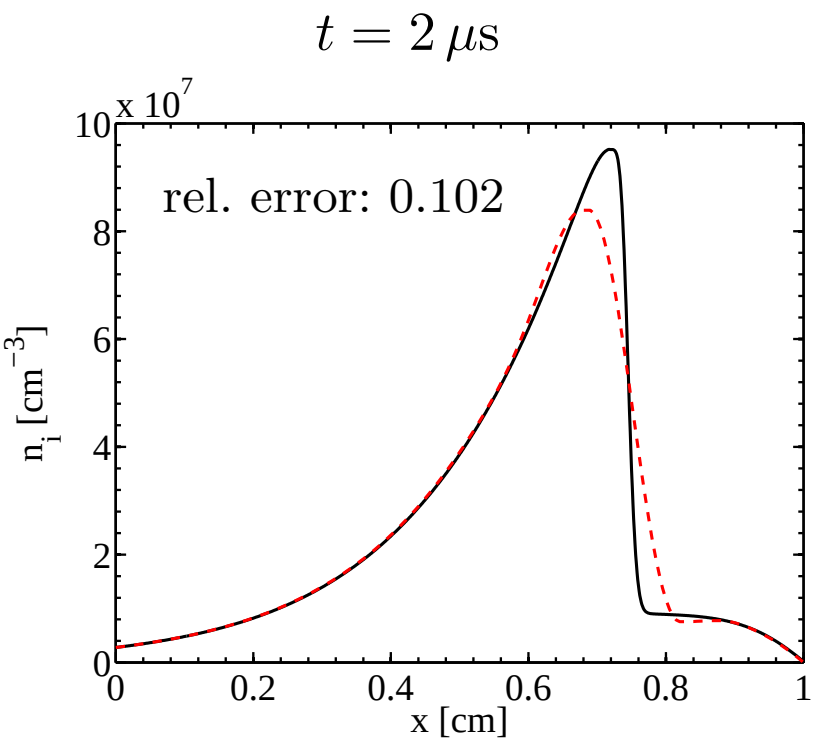

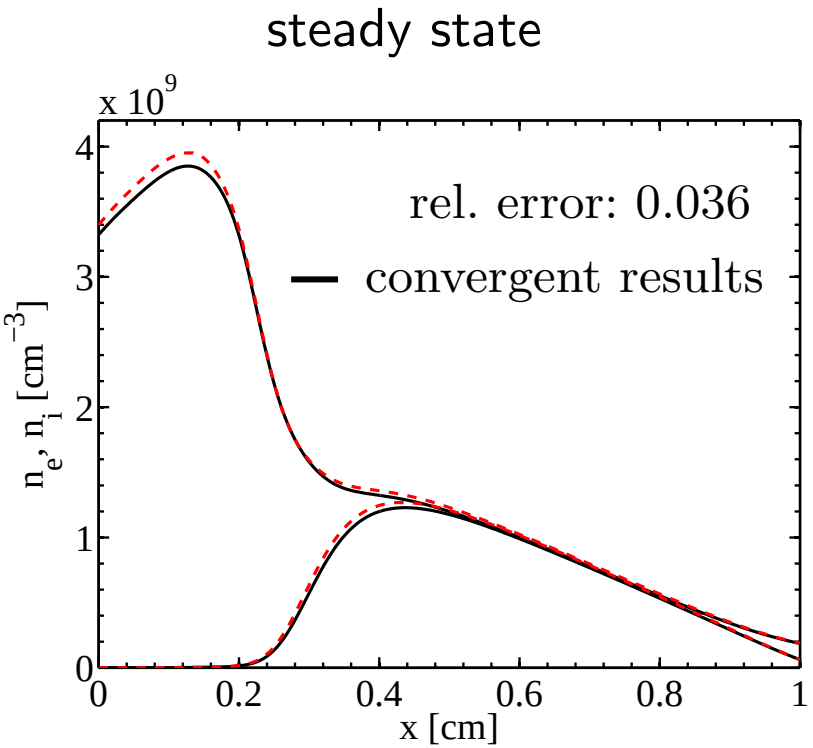

- Poor approximation of steep gradients
- No terracing effect due to additional artificial diffusion
- (Locally) fine spatial grids not applicable due to CFL restriction

FEMFCT (201 grid points)

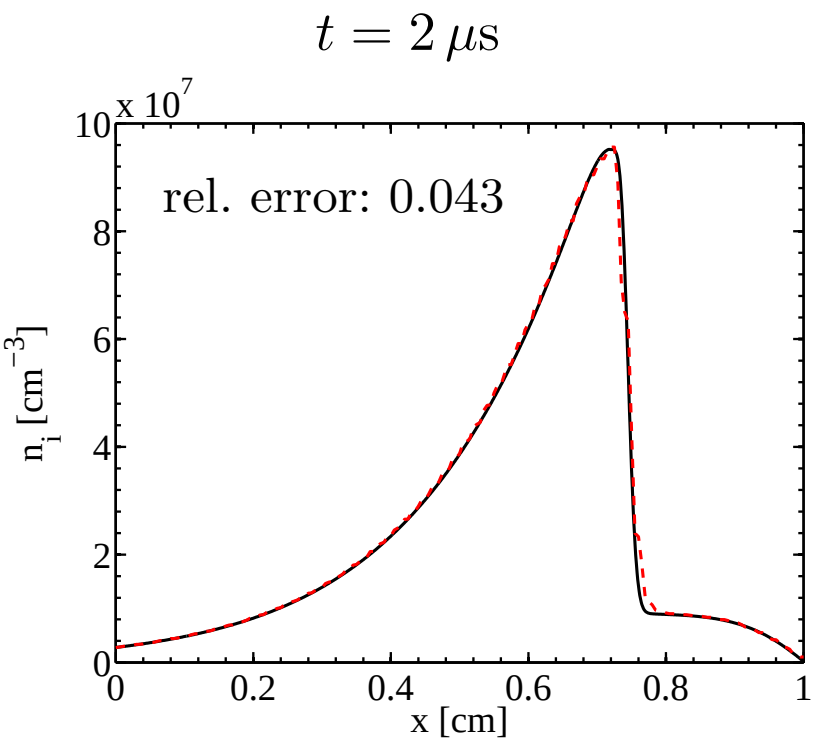

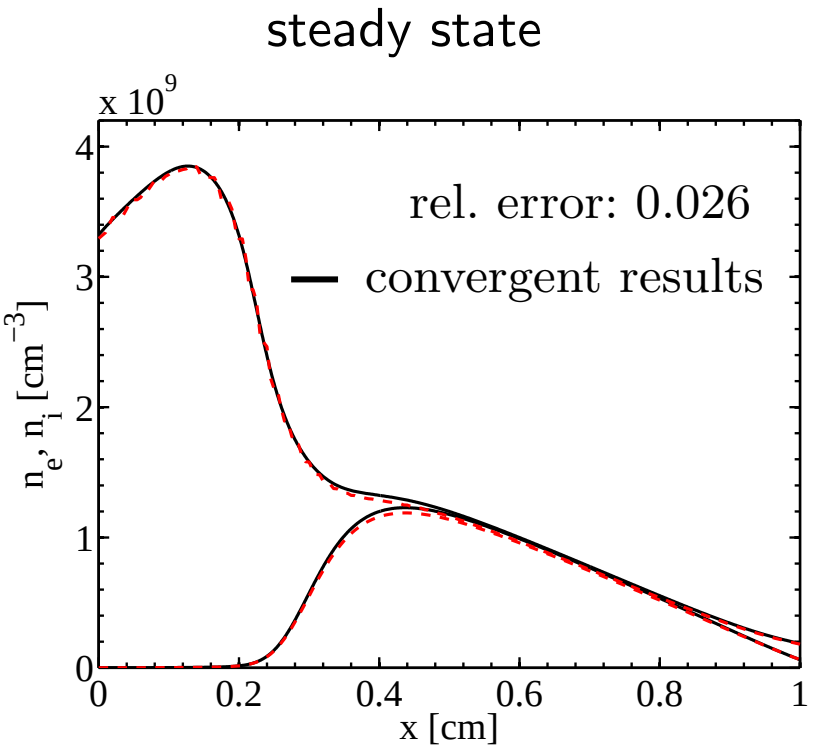

- Appearance of terraces at the front of steep gradients as well
- Apart from terraces, accurate results on coarse spatial grids
- (Local) grid refinement possible (no CFL restriction)

FEMFCT (201 grid points)

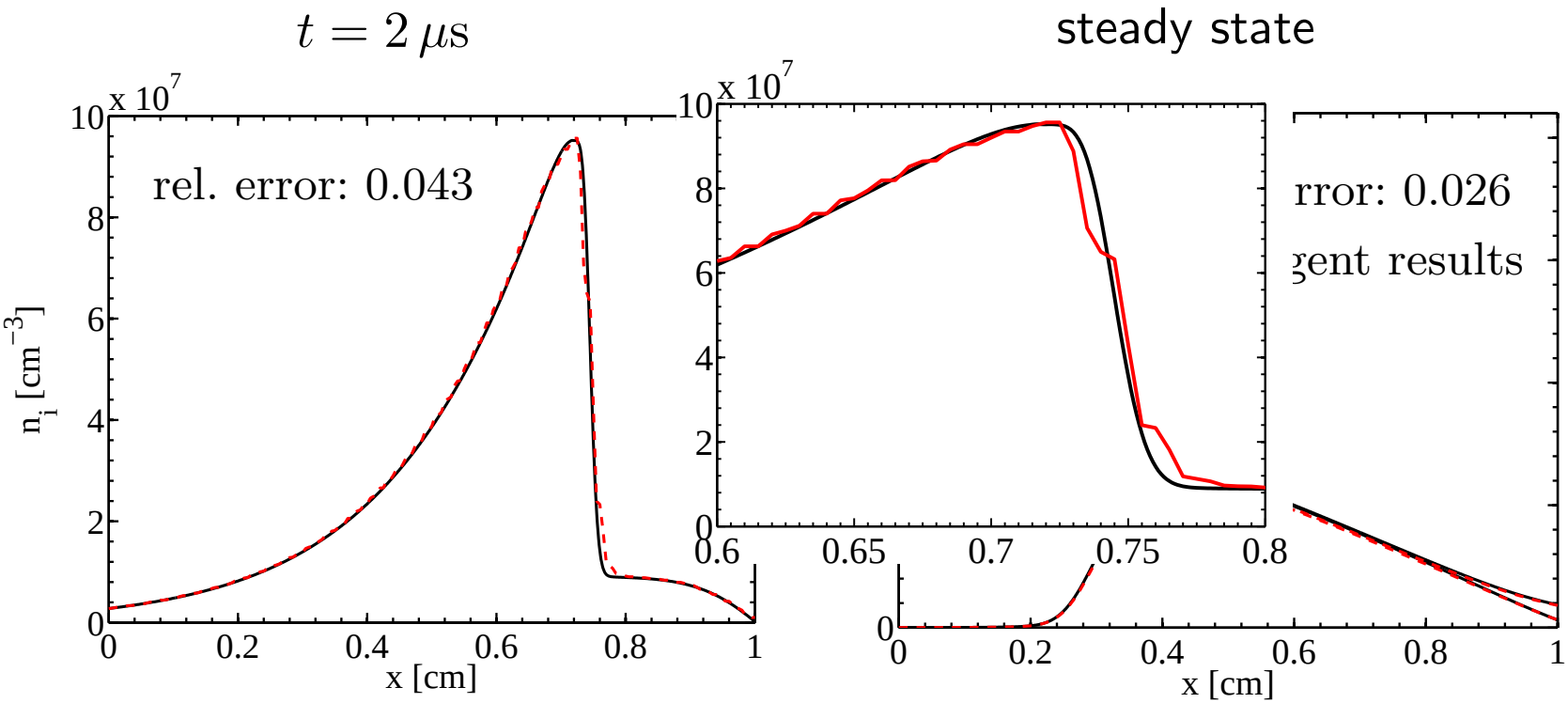

- Appearance of terraces at the front of steep gradients as well
- Apart from terraces, accurate results on coarse spatial grids
- (Local) grid refinement possible (no CFL restriction)

FEMFCT (201 grid points)

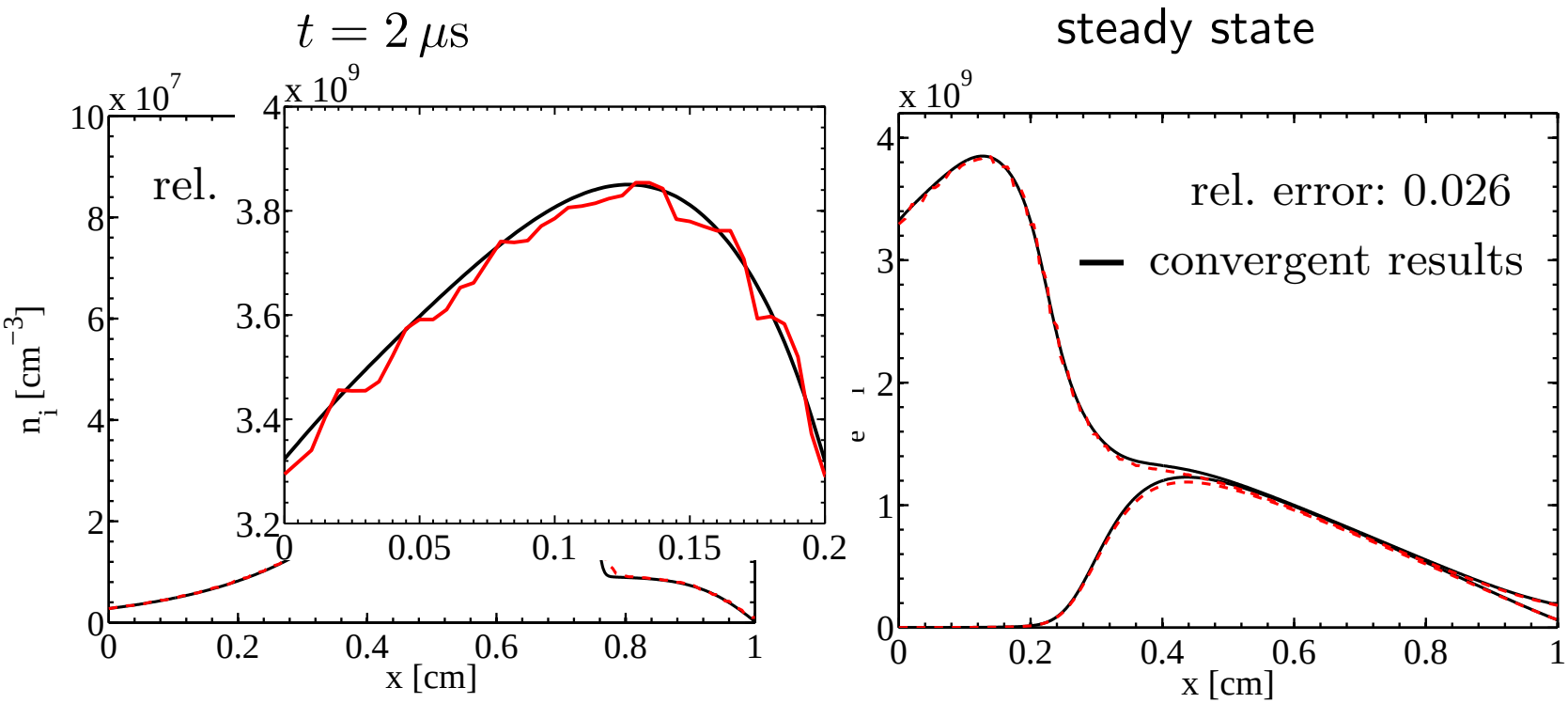

- Appearance of terraces at the front of steep gradients as well
- Apart from terraces, accurate results on coarse spatial grids
- (Local) grid refinement possible (no CFL restriction)

FEMFCT modified (201 grid points)

$t = 2\,\mu$s

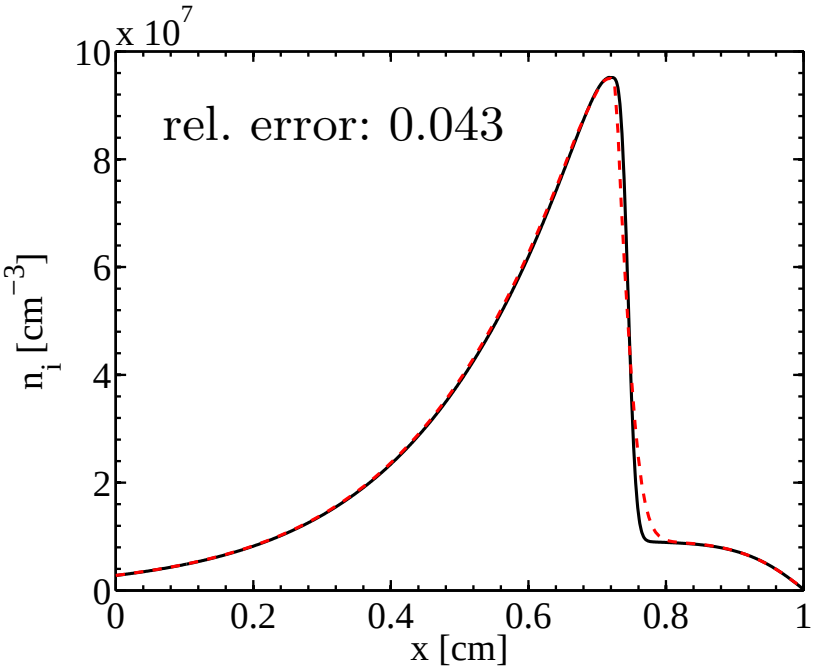

steady state

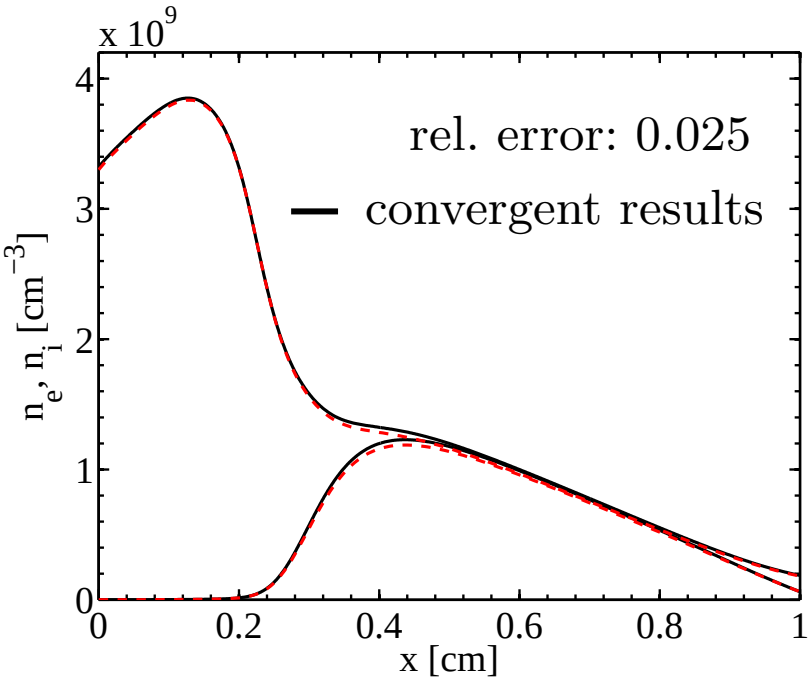

- No terracing effect
- Accurate results on coarse spatial grids
- (Local) grid refinement possible (no CFL restriction)

FEMFCT modified (201 grid points)

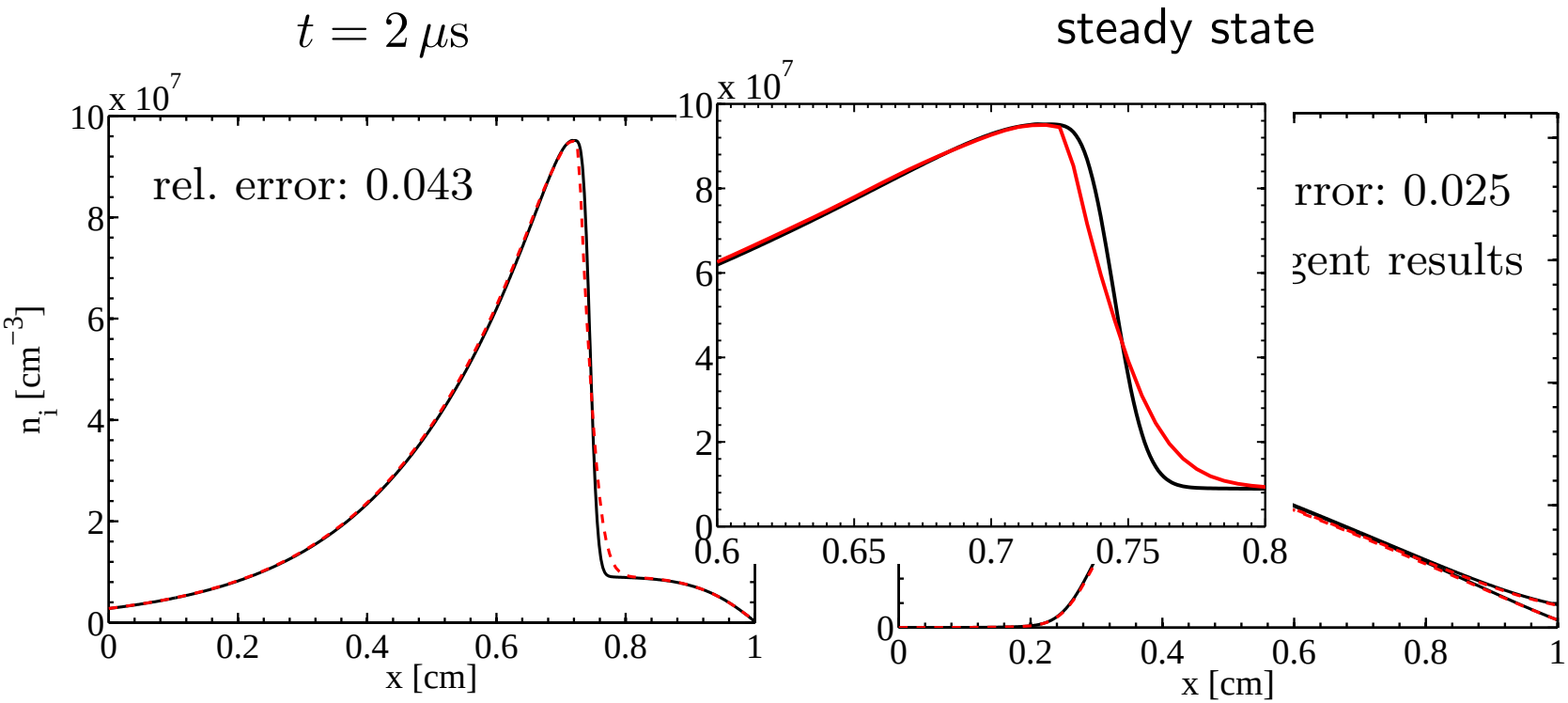

- No terracing effect
- Accurate results on coarse spatial grids
- (Local) grid refinement possible (no CFL restriction)

FEMFCT modified (201 grid points)

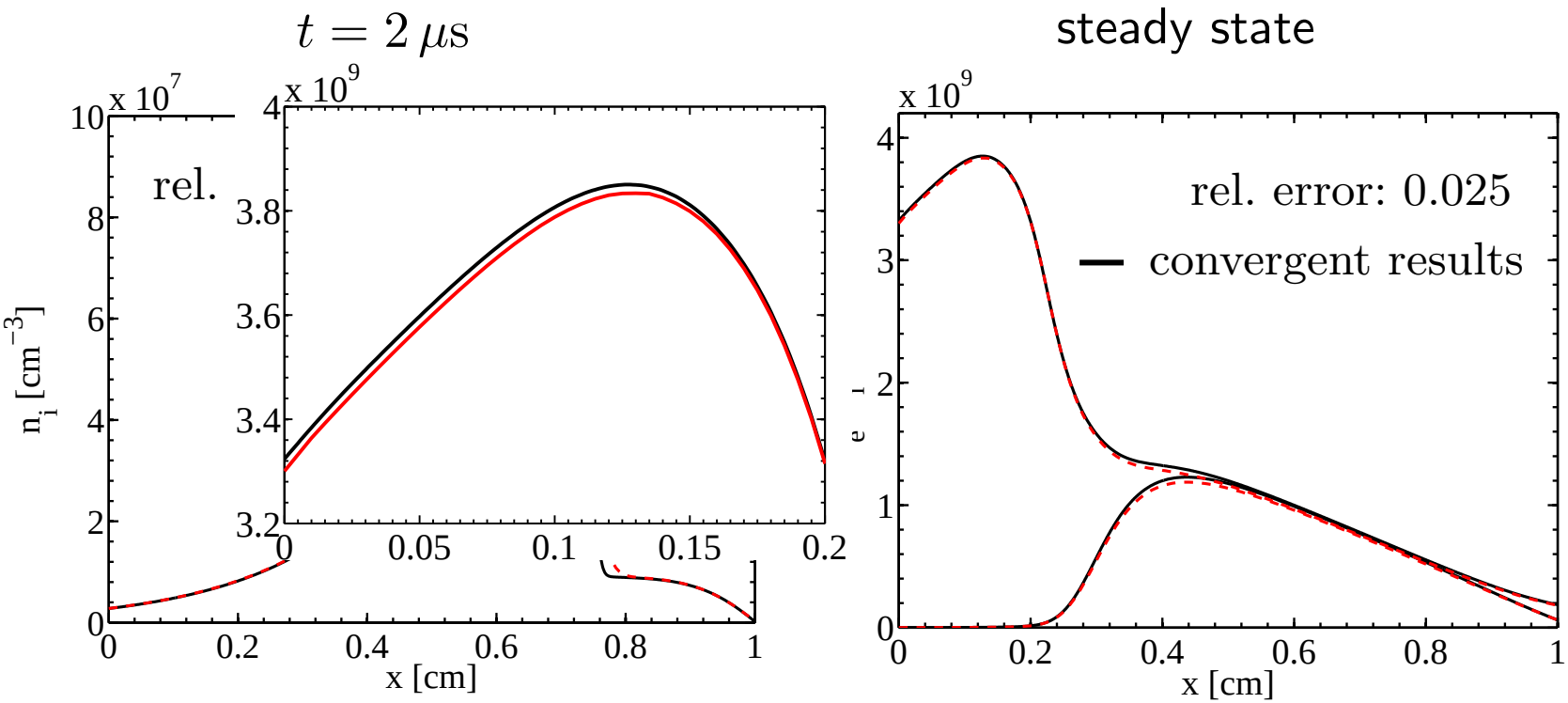

- No terracing effect
- Accurate results on coarse spatial grids
- (Local) grid refinement possible (no CFL restriction)

IFCT (201 gridpoints)

$t = 2\,\mu s$

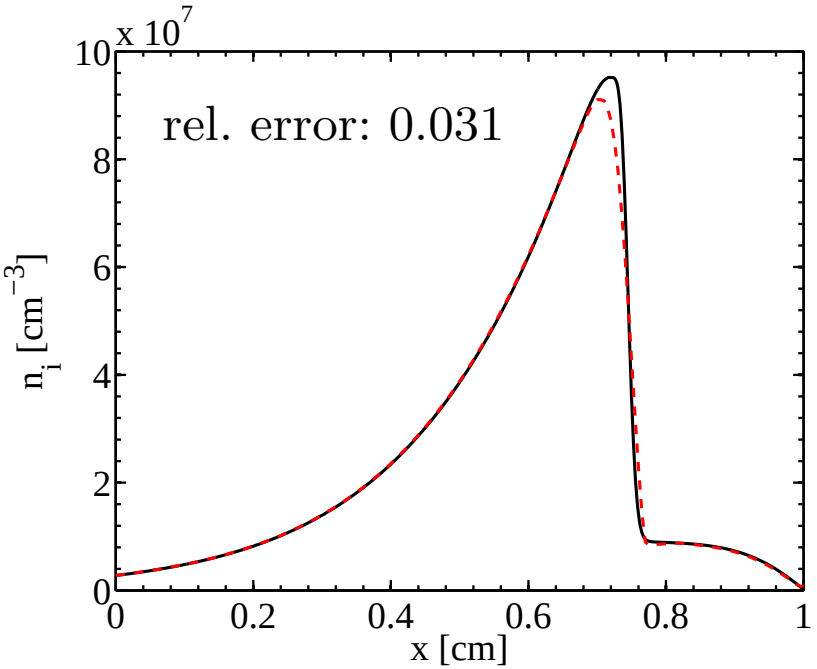

steady state

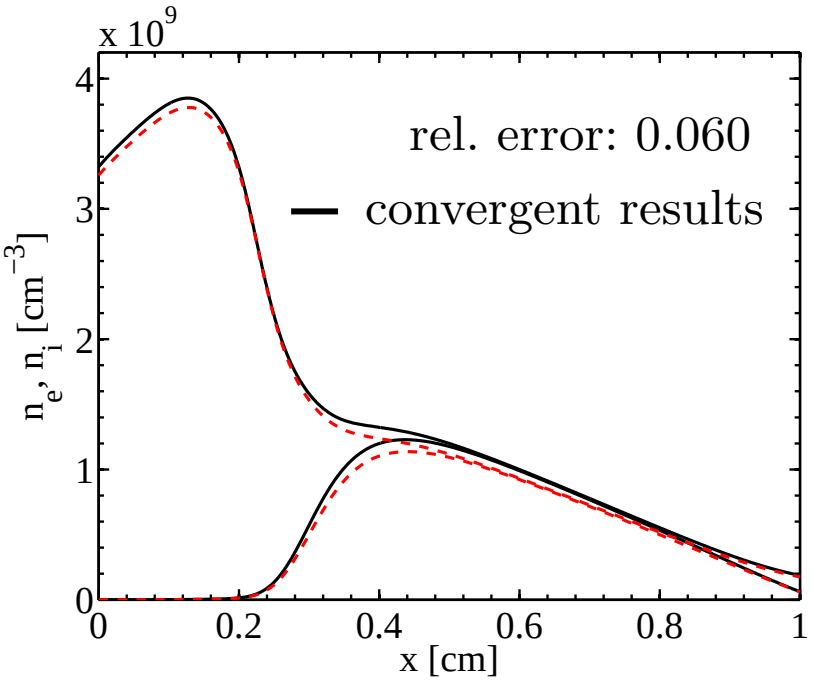

- No terracing effect
- Slightly higher errors at steady state
- (Local) grid refinement possible (no CFL restriction)

Summary & Outlook

- Investigation of hydrodynamic models for the theoretical description of low temperature plasmas
- Application of stabilized numerical methods
  - Petrov-Galerkin FEM for drift-diffusion model
  - FCT methods for strict hydrodynamic model
  - well suited to study gas discharges at low and atmospheric pressure
- New approach for hydrodynamic description under development
- Extension of the model to 2D/3D geometries planed

Kontakt

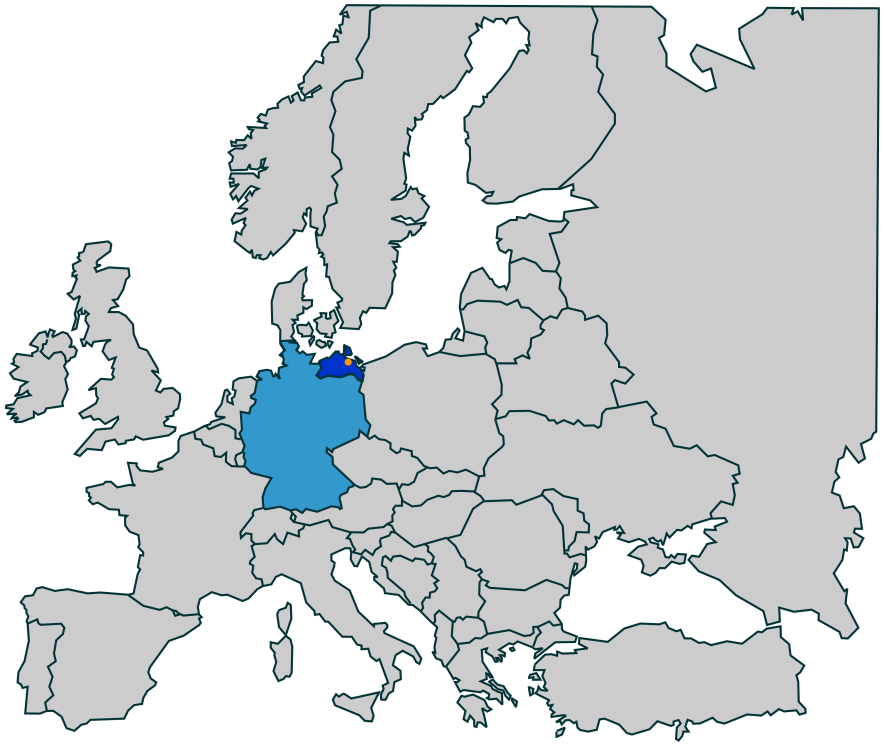

Leibniz-Institut für Plasmaforschung und Technologie e.V.
Adresse: Felix-Hausdorff-Str. 2, 17489 Greifswald
Telefon: +49 - 3834 - 554 300, Fax: +49 - 3834 - 554 301
E-mail: welcome@inp-greifswald.de, Web: www.inp-greifswald.de

Discharge configuration

- 1D model with electrode gap $d = 1.5\,\mathrm{mm}$
- Dielectric: Al_2O_3, $\varepsilon_r = 10$, $D = 0.5\,\mathrm{mm}$
- Sinusoidal applied voltage ($f = 60\,\mathrm{kHz}$)
- Gas: argon
- Pressure $p = 1\,\mathrm{atm}$
- Gas temperature $T_{gas} = 300\,\mathrm{K}$

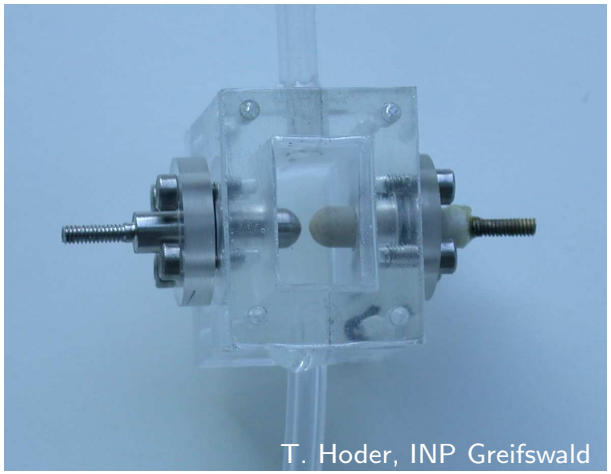

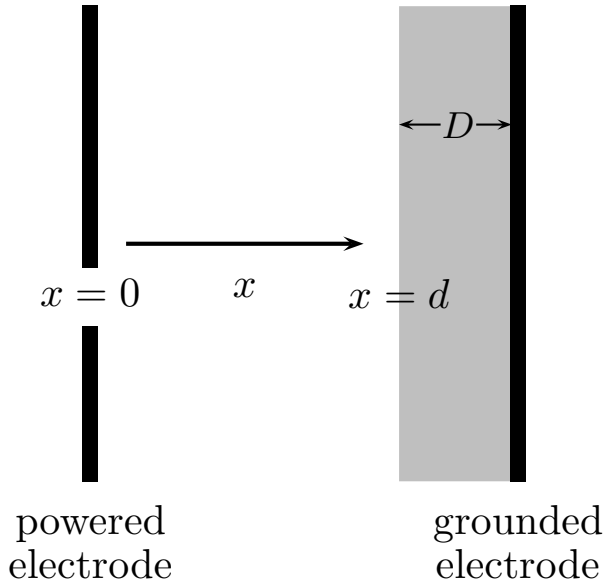

Reaction kinetics

- Considered species: electrons, Ar^+ and Ar_2^+ ions, 11 excited states
- About 100 collisional and radiative processes

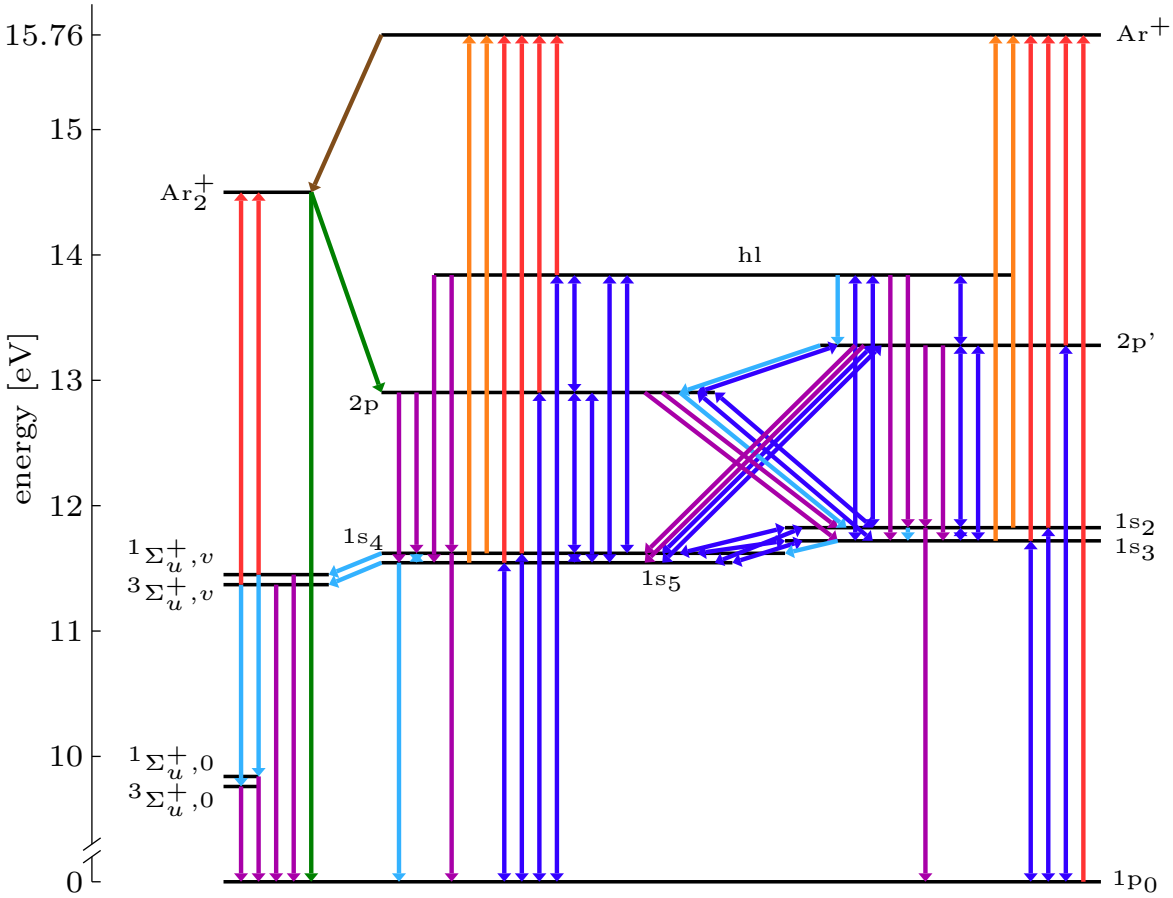

Electron collision processes:
excitation/de-excitation
ionization
recombination

Collisions between heavy particles:
chemo-ionization
charge transfer reactions
quenching

Radiative processes

Current-voltage characteristics

- Discharge behaviour depends sensitively on applied voltage
- Two different discharge modes at applied voltages $< 3\,\mathrm{kV}$
- Periodic behaviour at higher voltages

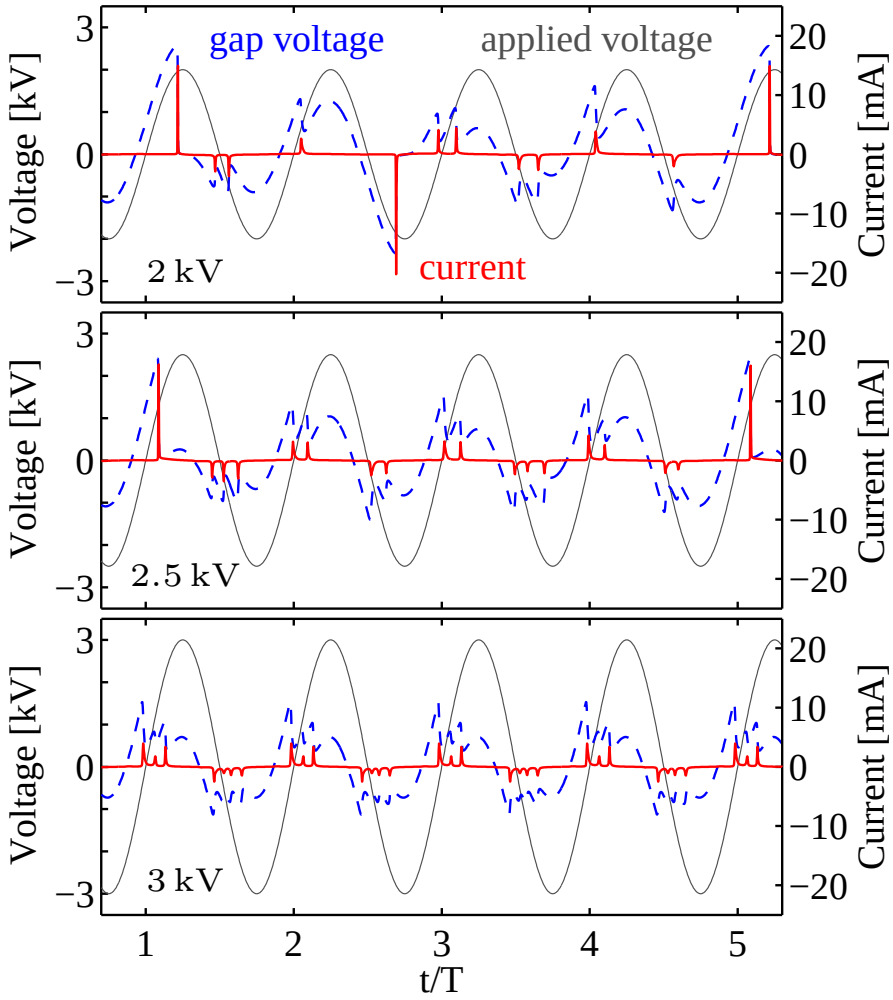

Period multiplication phenomena

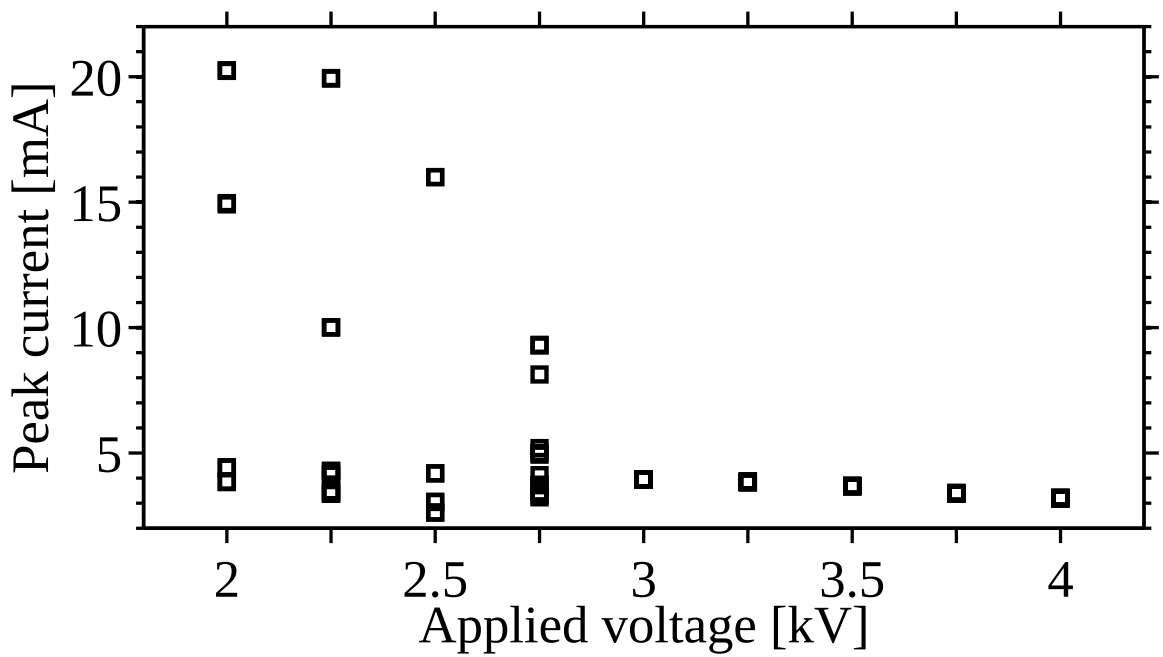

- Period multiplication phenomena occur at $V_0 < 3\,\mathrm{kV}$
- Decrease of maximum current peak value at increasing voltage because of higher memory voltage $\Phi_\mathrm{m} = \Phi_\mathrm{a} - \Phi_\mathrm{gap}$

Period multiplication phenomena

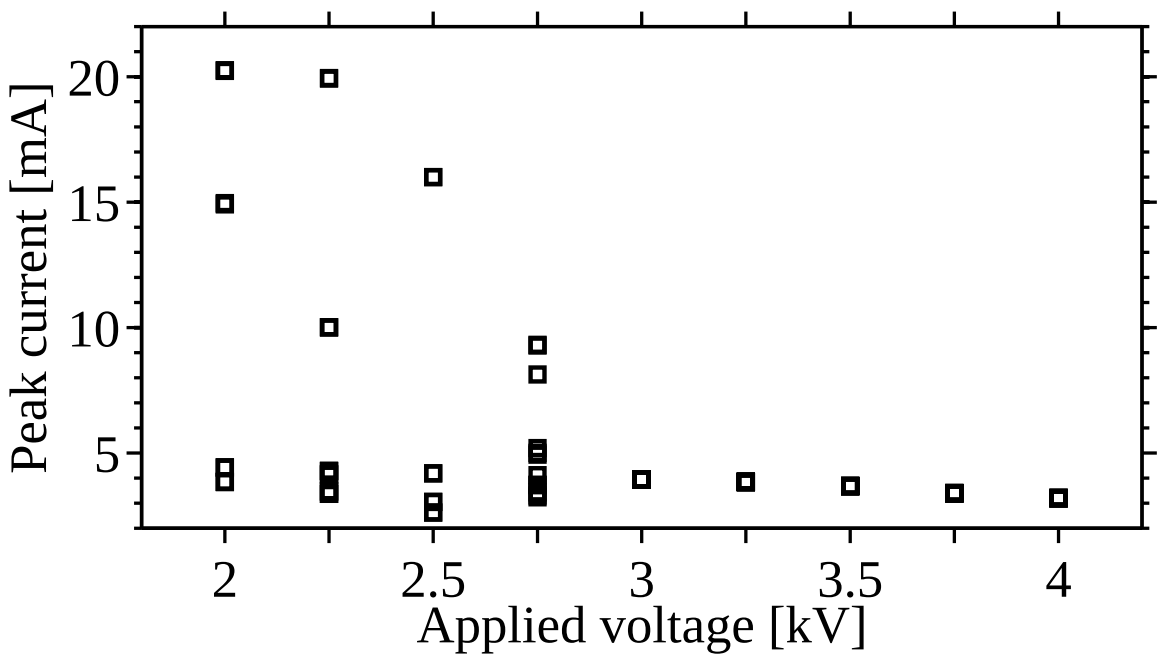

- Chaotic (non-periodic) behaviour around $V_0 = 2.75\,\mathrm{kV}$
- Periodic conditions at $V_0 > 3\,\mathrm{kV}$

Period multiplication phenomena

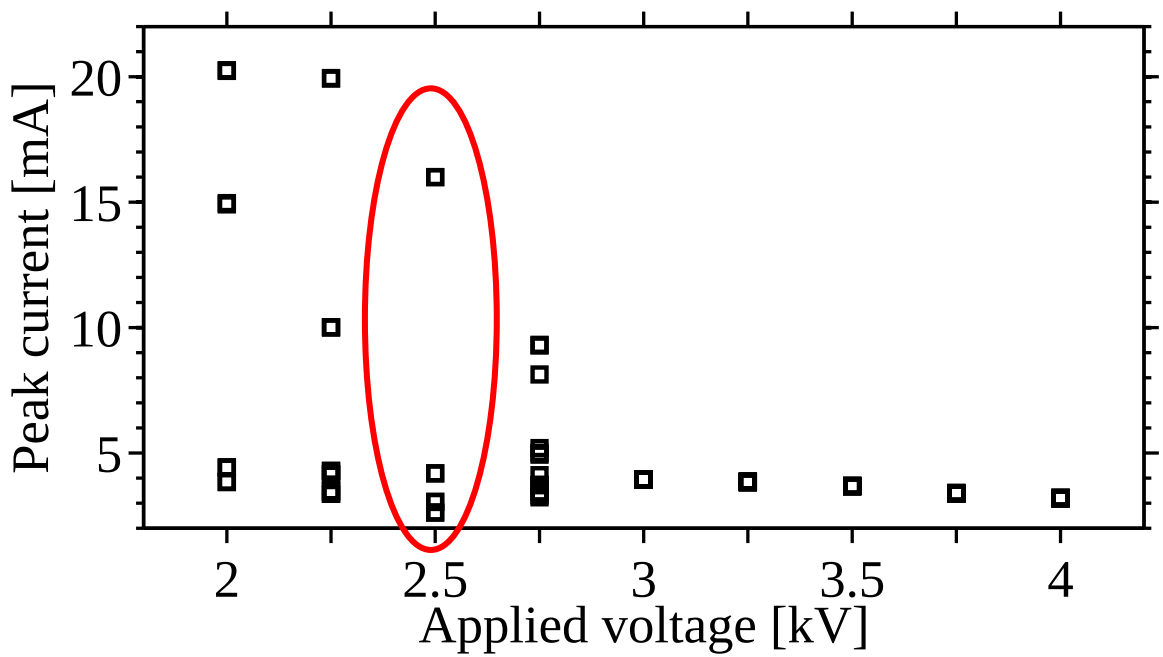

- Chaotic (non-periodic) behaviour around $V_0 = 2.75\,\mathrm{kV}$
- Periodic conditions at $V_0 > 3\,\mathrm{kV}$
- Analysis of discharge behaviour at $V_0 = 2.5\,\mathrm{kV}$

Period multiplication at $V_0 = 2.5\,\mathrm{kV}$

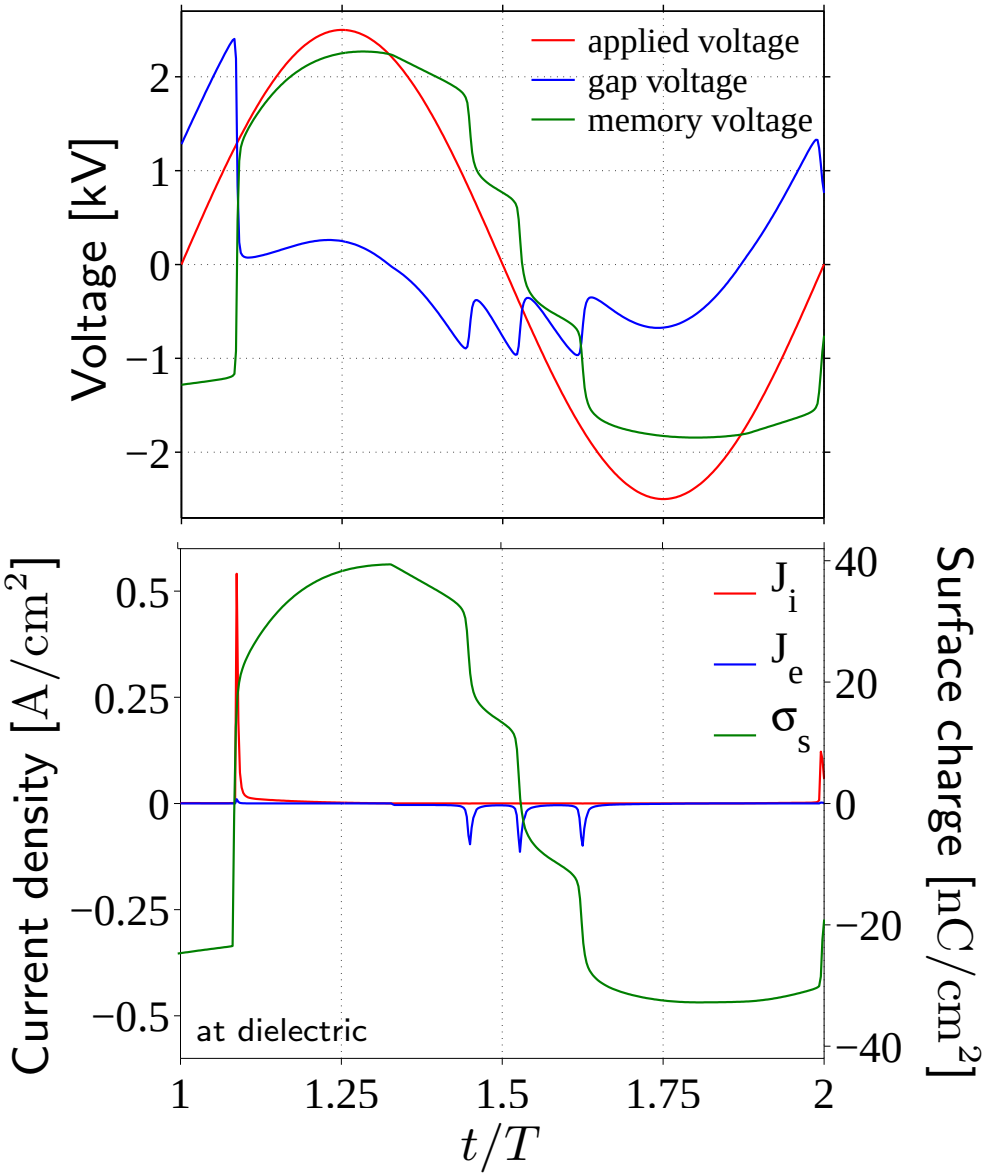

- High ignition voltage at first discharge event
- Multiple weaker discharges with lower ignition voltage after change of polarity
- Last discharge event not equal to the first due to higher memory voltage

Period multiplication at $V_0 = 2.5\,\mathrm{kV}$

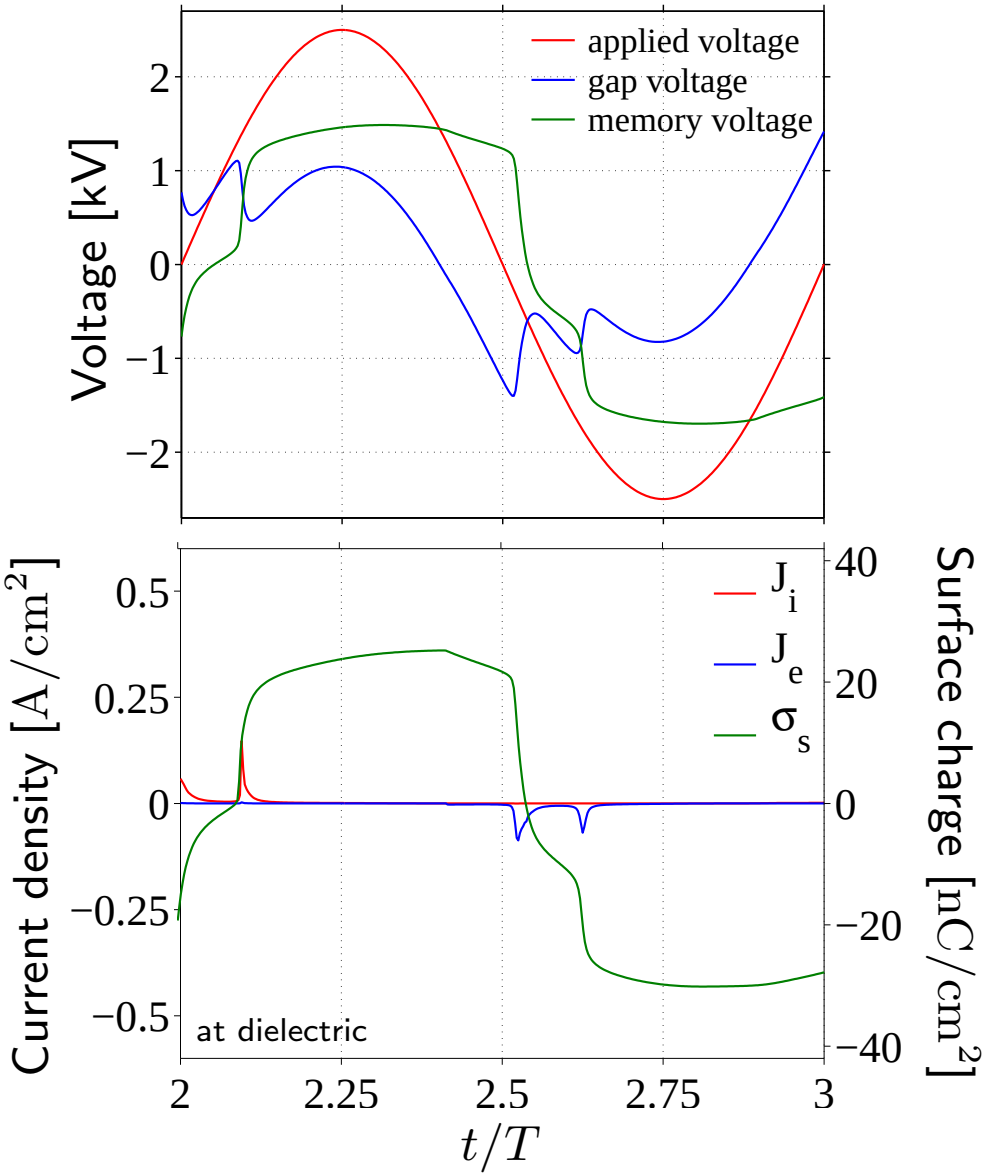

- Sequence of weaker discharges events with two or three current peaks

Period multiplication at $V_0 = 2.5\,\mathrm{kV}$

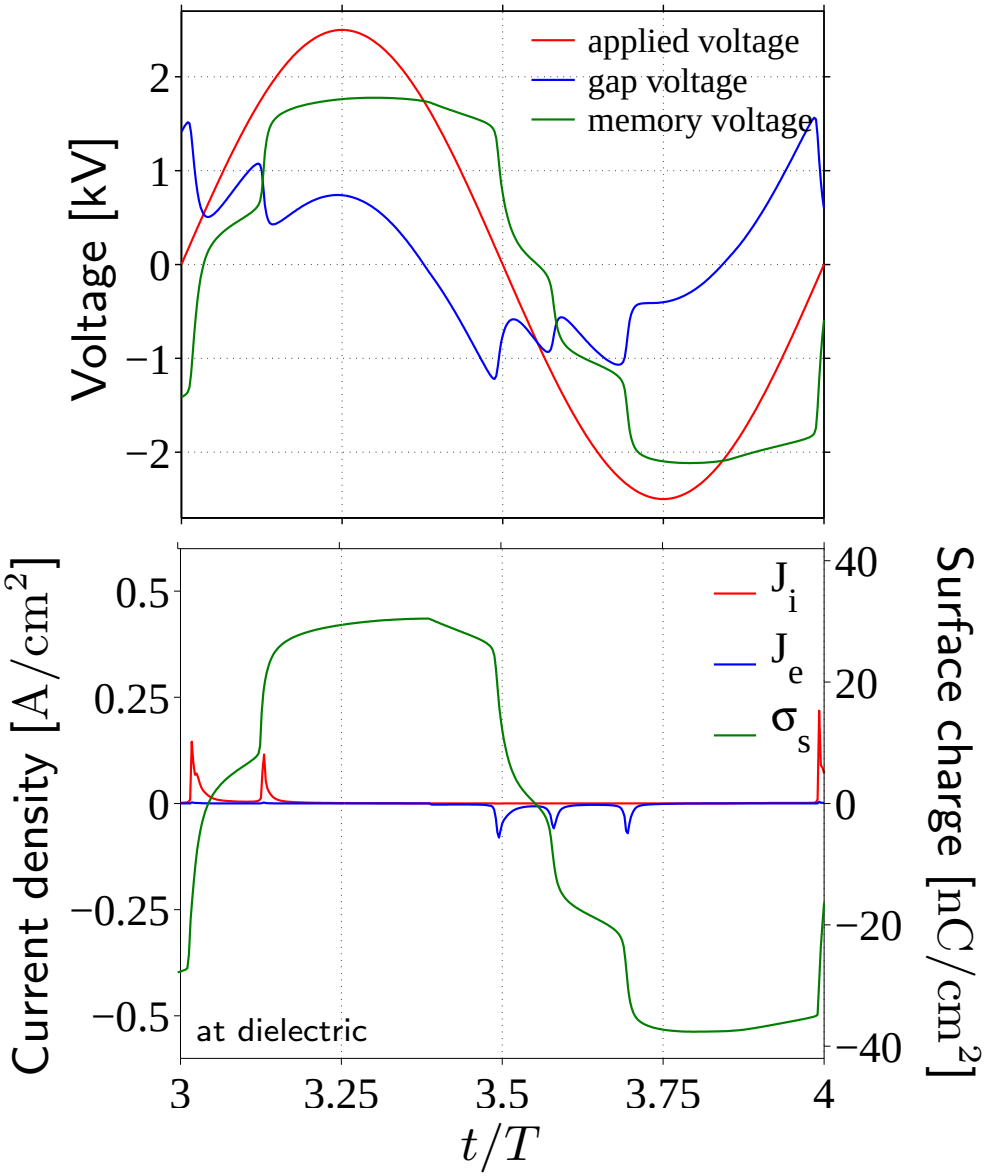

- Sequence of weaker discharges events with two or three current peaks

Period multiplication at $V_0 = 2.5\,\mathrm{kV}$

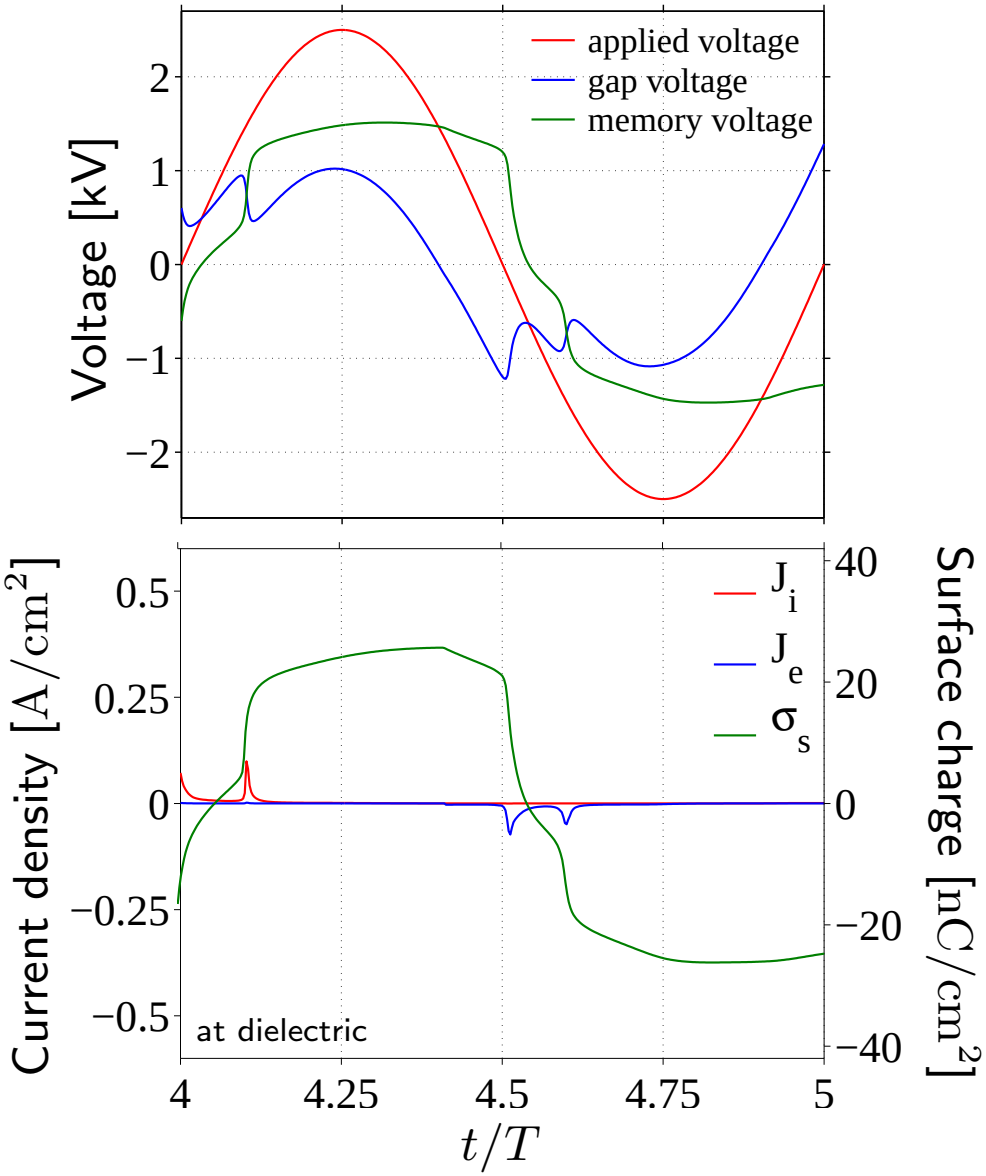

- Transition to the same conditions after four periods

Period multiplication at $V_0 = 2.5\,\mathrm{kV}$

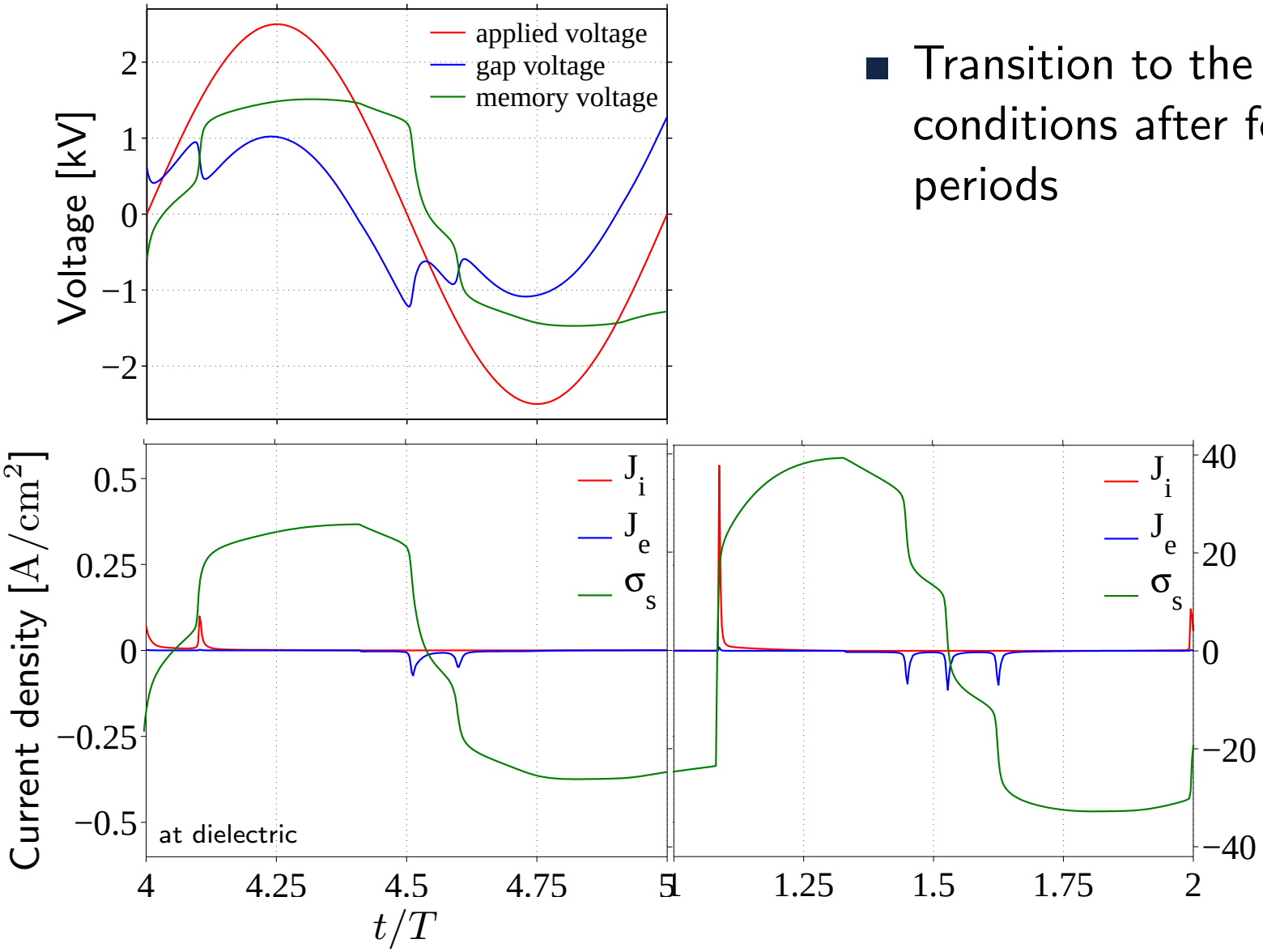

- Transition to the same conditions after four periods

Period multiplication at $V_0 = 2.5\,\mathrm{kV}$

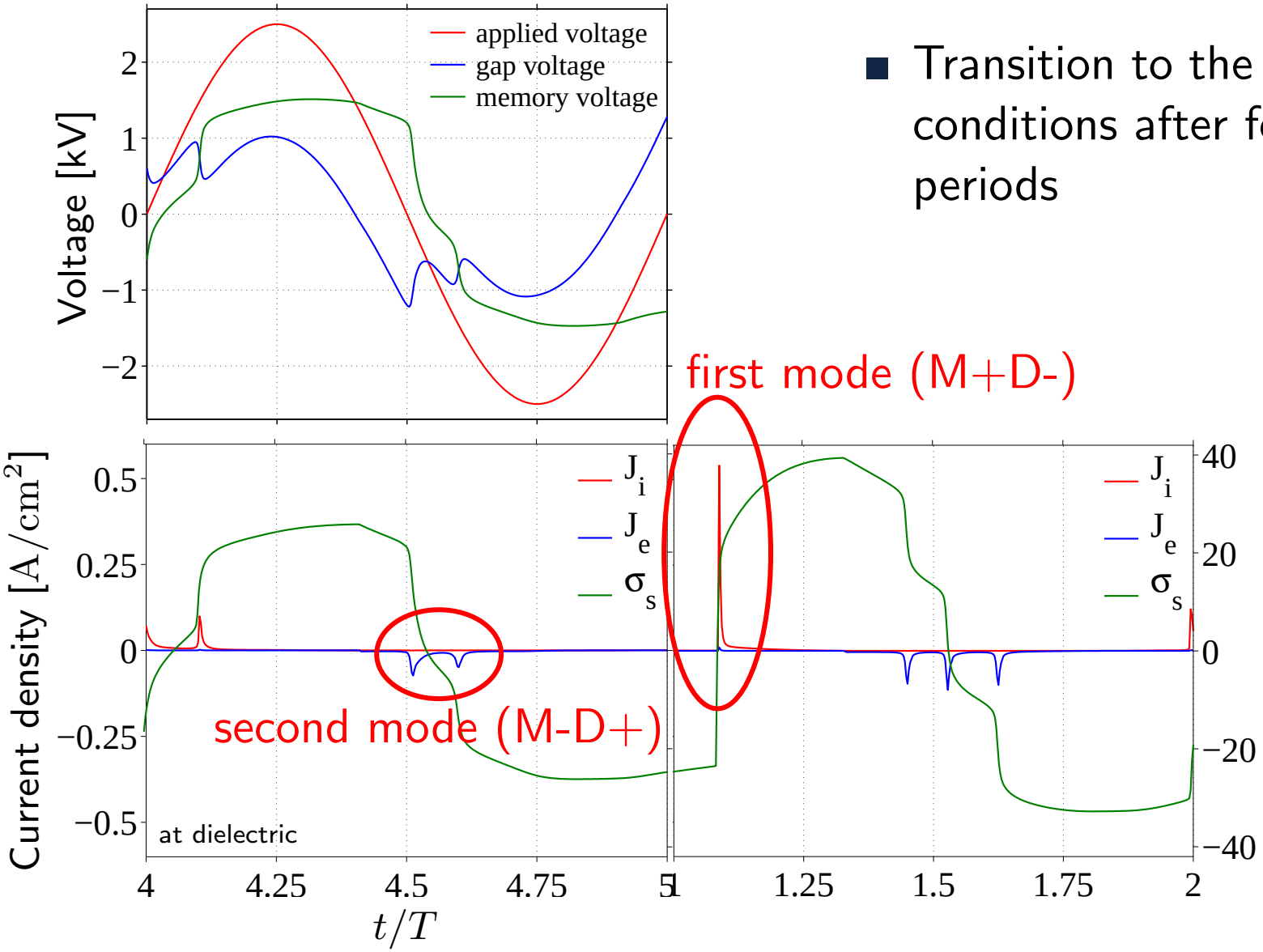

- Transition to the same conditions after four periods

Spatiotemporal discharge behaviour ($V_0 = 2.5\,\mathrm{kV}$)

First discharge mode

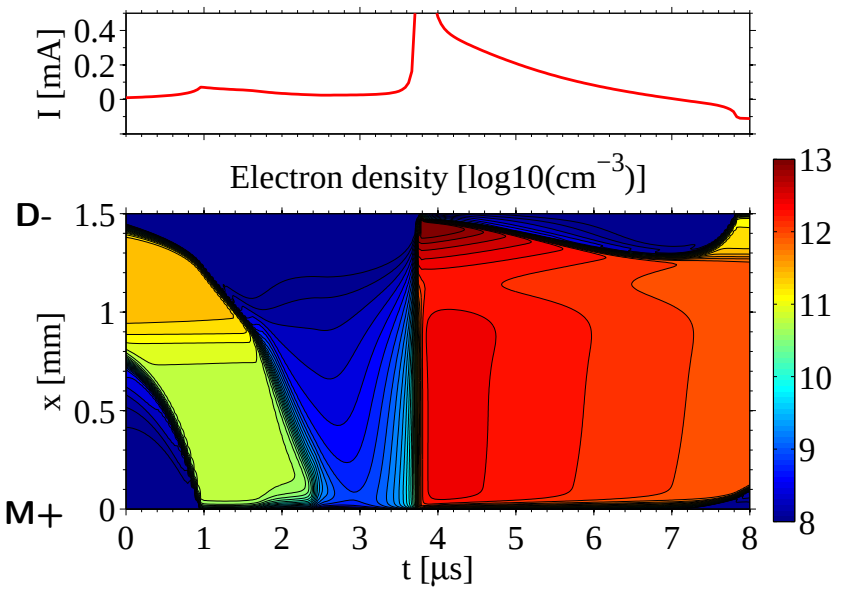

Second discharge mode

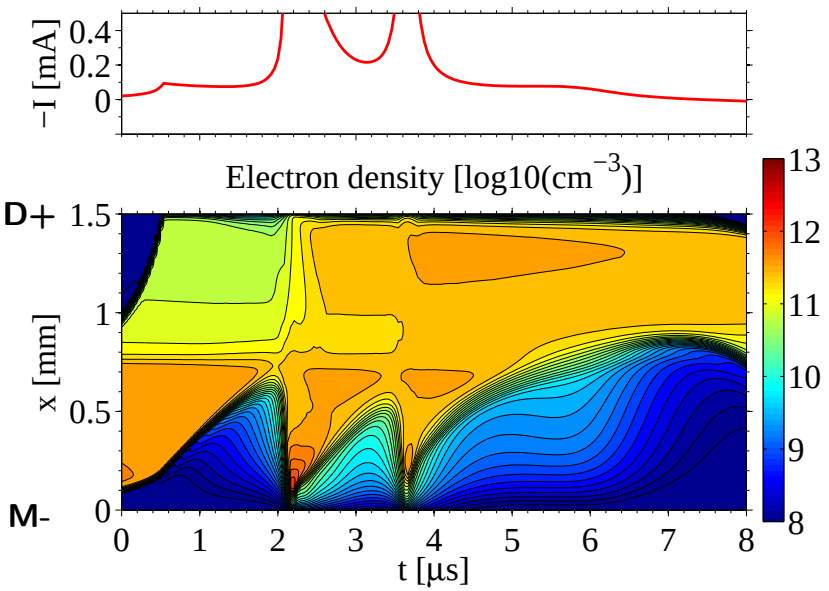

- Low electron density before ignition of microdischarges in first discharge mode (single current peak)
- Electron density locally high before ignition of microdischarges in second discharge mode (multiple current peaks)

Charge carrier densities at current peaks ($V_0 = 2.5\,\mathrm{kV}$)

First discharge mode

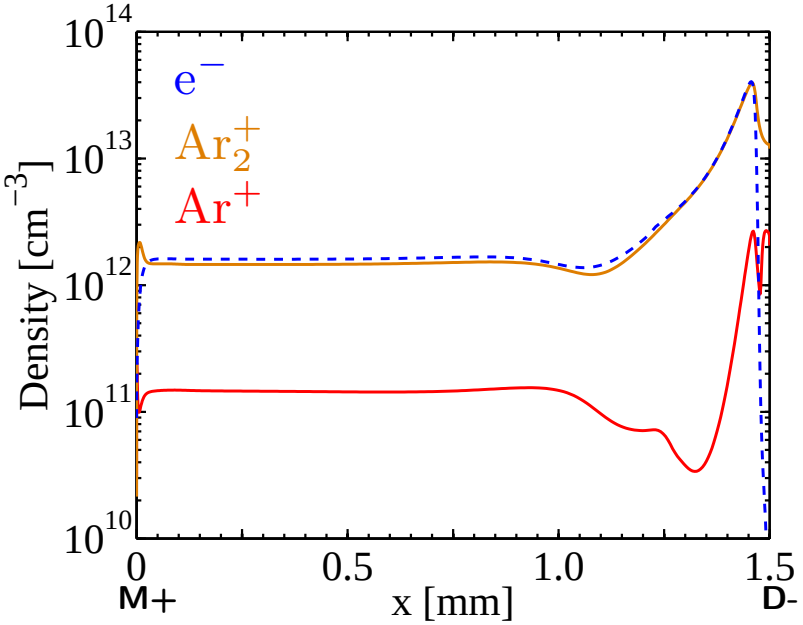

Second discharge mode

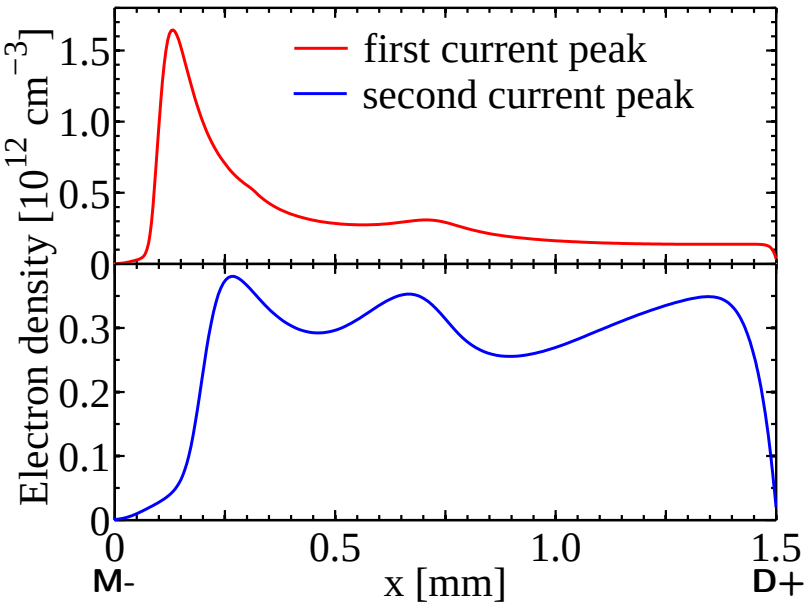

- Glow-discharge-like spatial structure in first discharge mode
- Second discharge mode is characterized by an inhomogeneous positive column

Analysis of the electron budget (discharge centre, $V_0 = 2.5\,\mathrm{kV}$)

First discharge mode

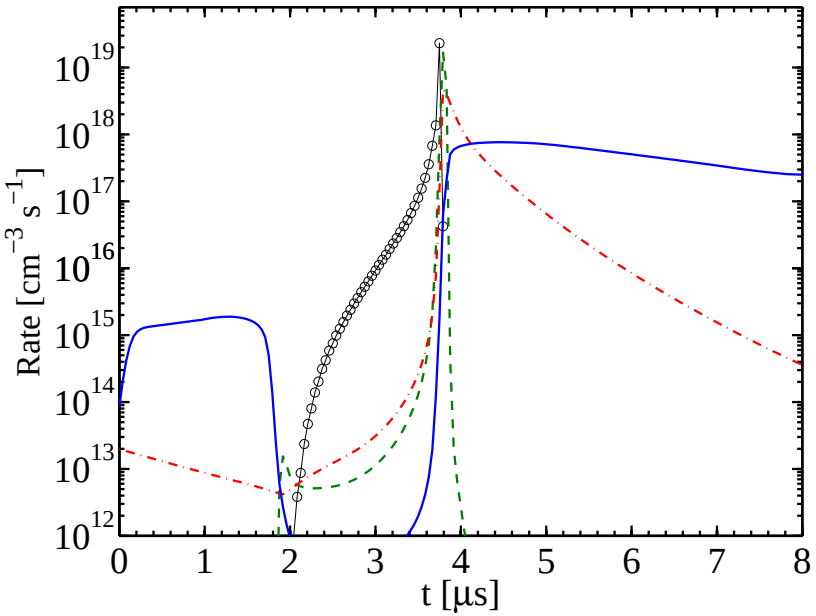

Second discharge mode

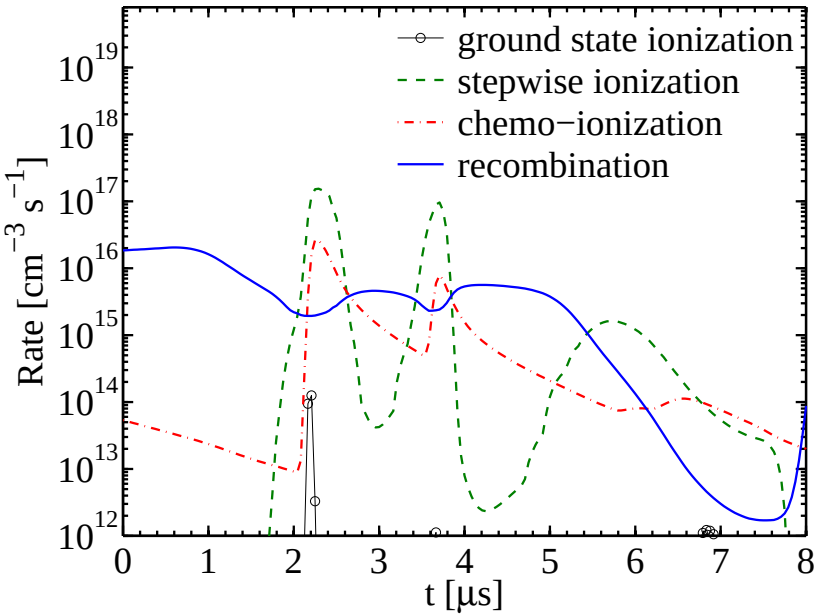

- Townsend-like phase initiates the discharge ignition in first discharge mode
- Charge carrier production results mainly from stepwise ionization in second discharge mode

Discharge configuration

- Spatially one-dimensional model, gap $d = 1\,\mathrm{cm}$
- Gas: argon
- Gas temperature $T_\mathrm{g} = 300\,\mathrm{K}$, pressure $p = 760\,\mathrm{Torr}$
- Applied voltage pulse $U_0 = 25\,\mathrm{kV}$, $100\,\mathrm{ns}$
- Discharge voltage from electrical circuit equations

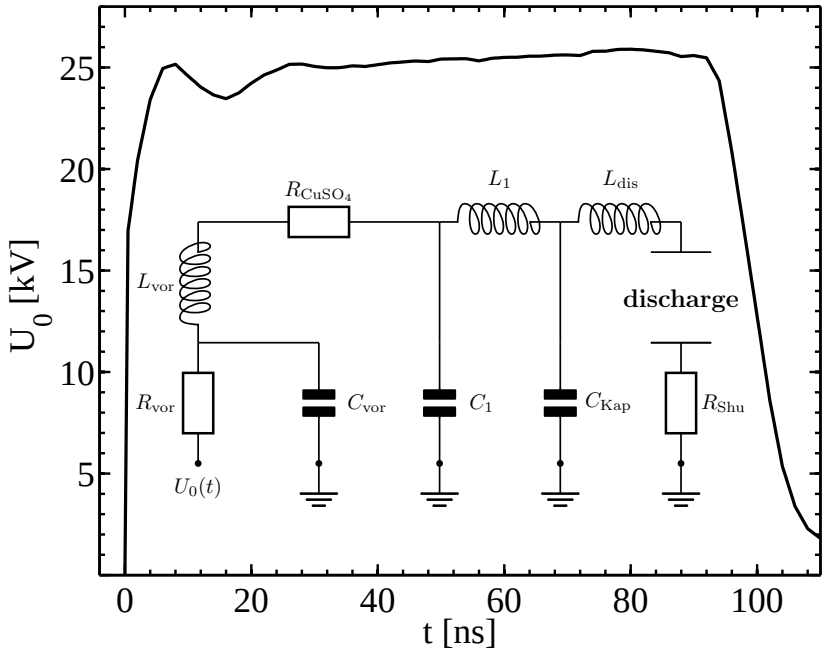

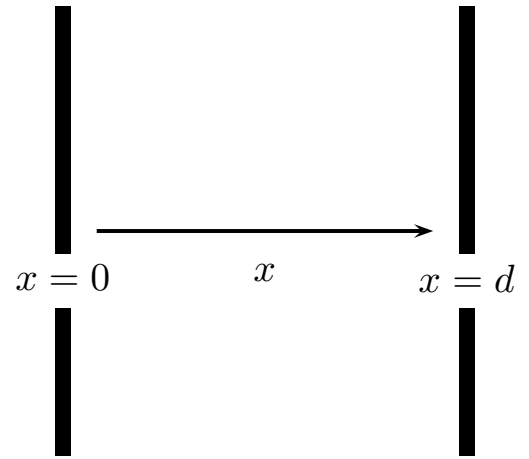

powered electrode

$\Phi(0,t) = U_\mathrm{dis}(t)$

grounded electrode

$\Phi(d,t) = 0$

Discharge characteristics

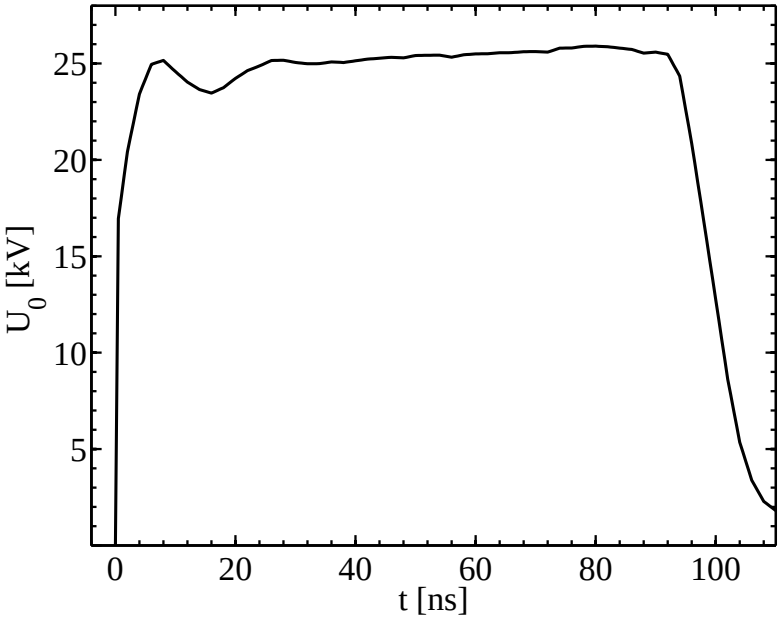

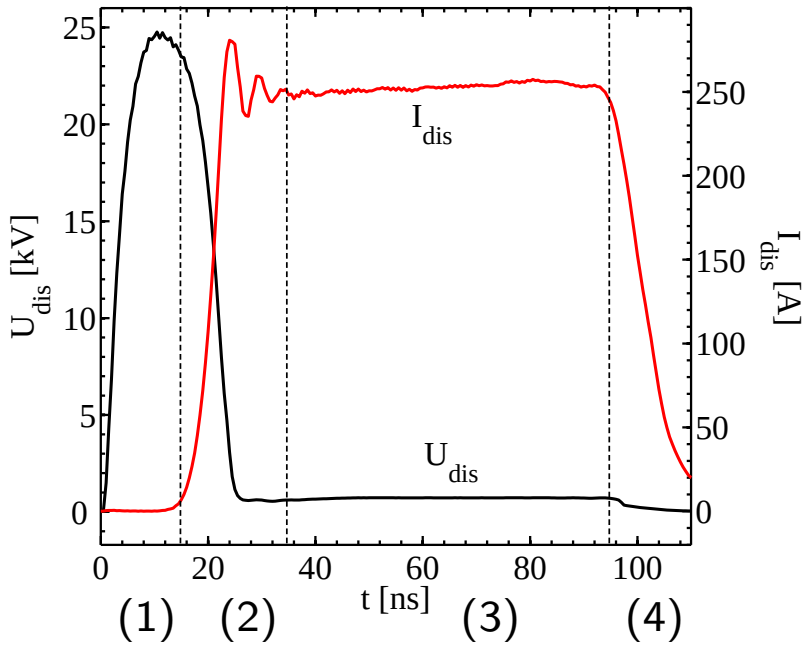

- t $<$ 15 ns: Townsend phase (1)
- 15–35 ns: ignition phase (2)
- 35–95 ns: quasi-steady-state (3)
- t $>$ 95 ns: recombination phase (4)

Spatiotemporal behaviour

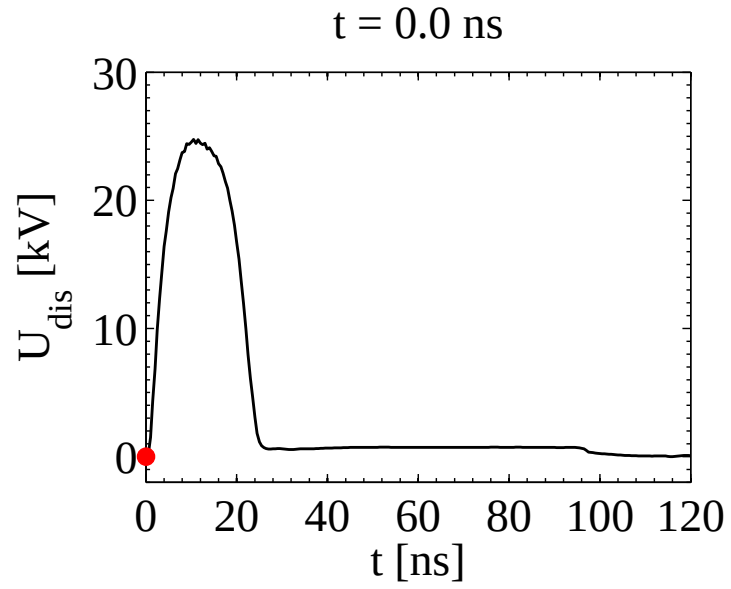

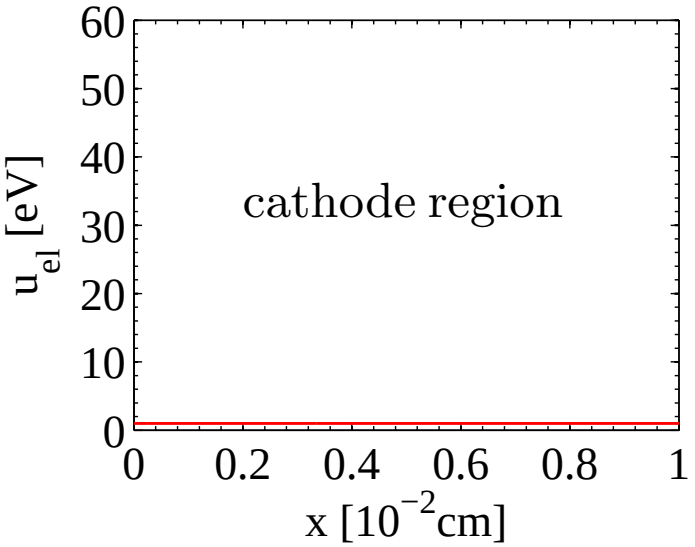

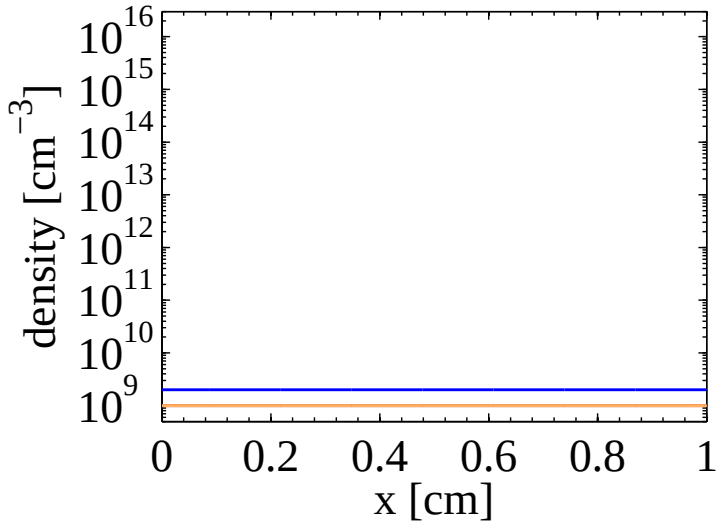

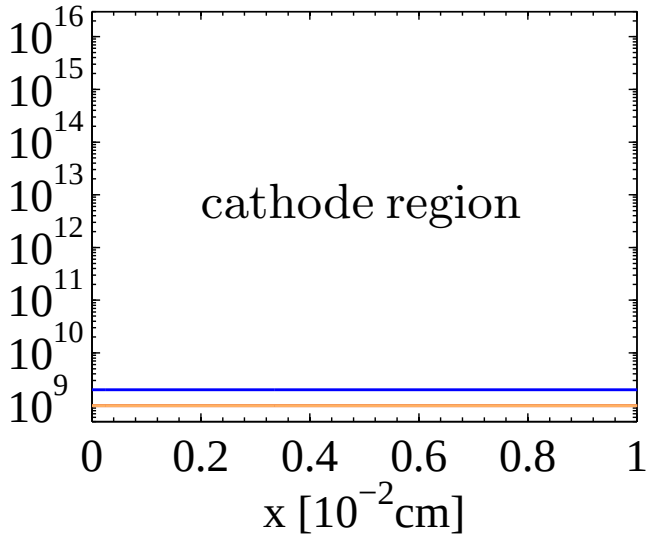

Ar^+

Ar_2^+

e^-

Spatiotemporal behaviour

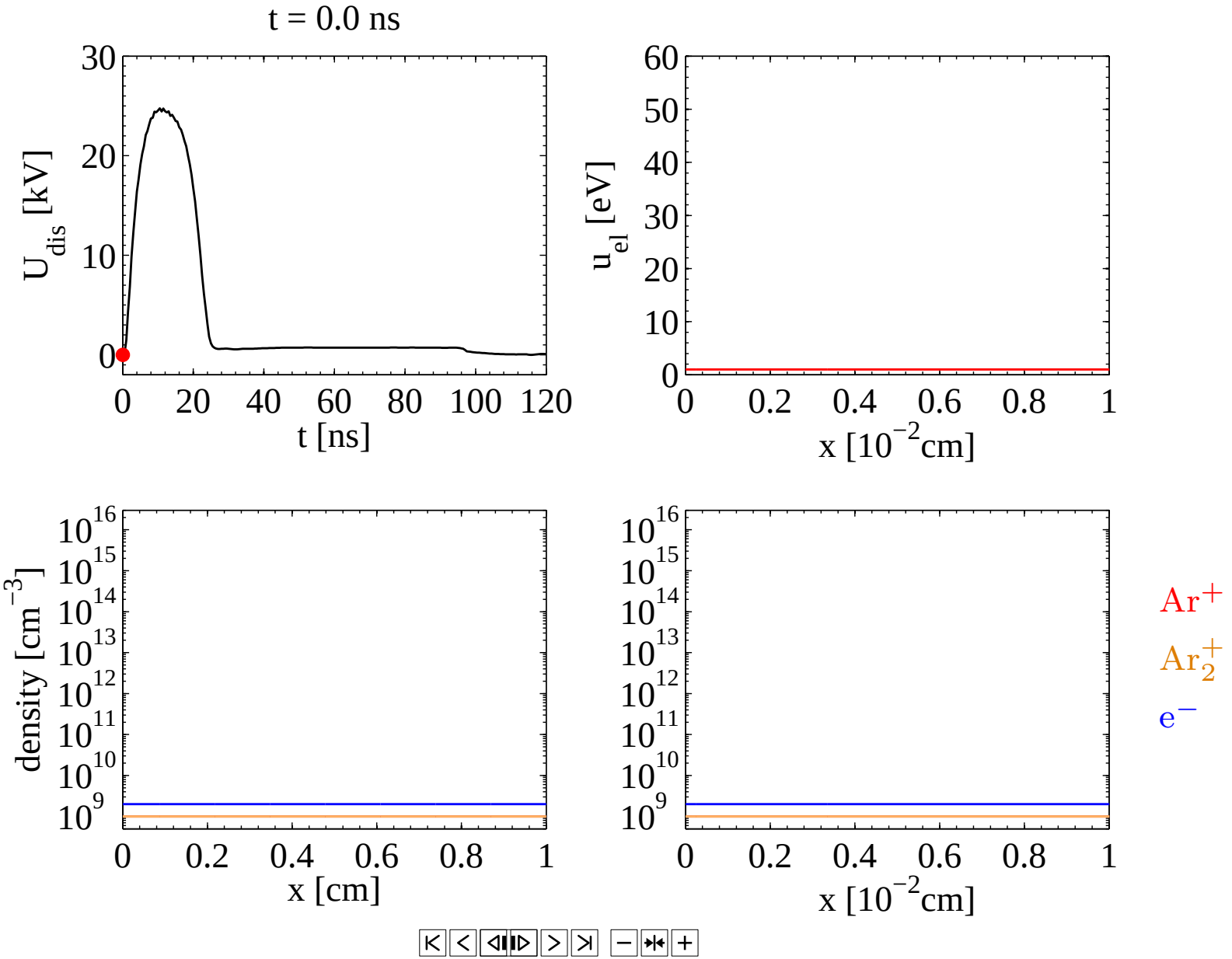

Analysis of the electron budget (discharge centre)

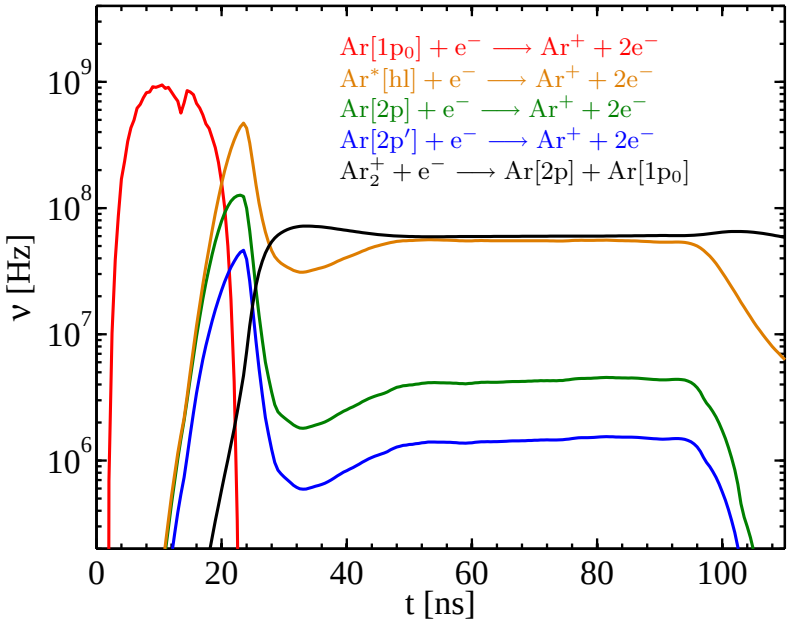

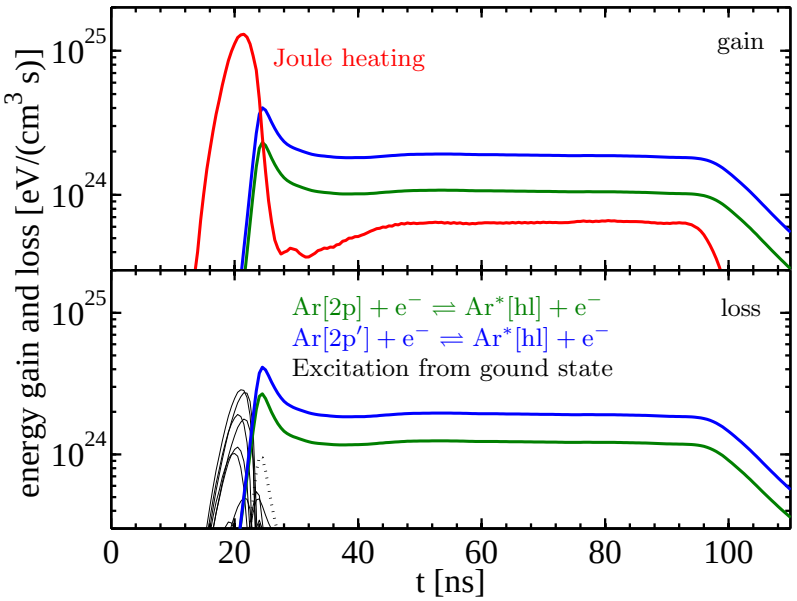

- Ionisation from ground state dominates electron production during Townsend phase
- During ignition phase stepwise ionisation from higher excited states become important
- Collisions with $\mathrm{Ar}[2\mathrm{p}]$, $\mathrm{Ar}[2\mathrm{p}']$ and higher excited states dominate power budget in the quasi-steady state

Quasi-steady state

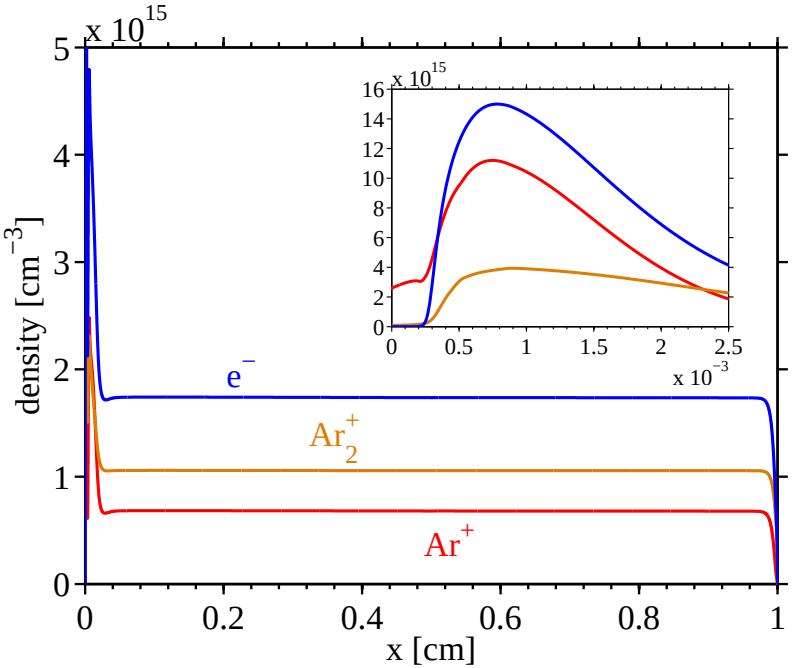

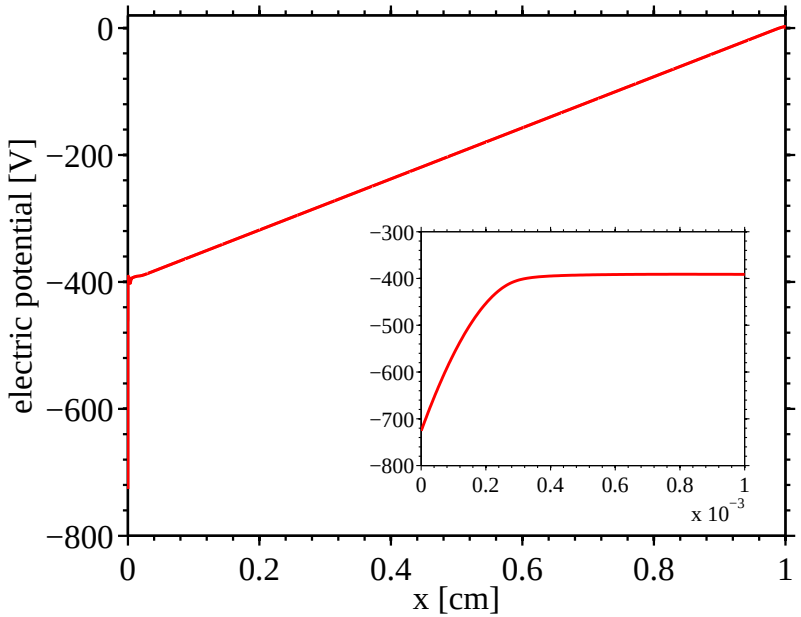

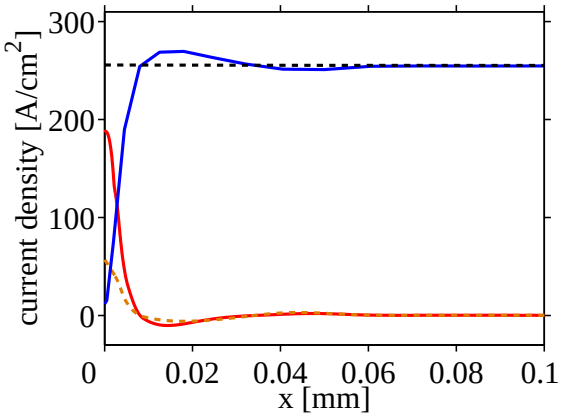

- Similarity parameters agree well with similarity laws for normal glow discharges

$$p\,d_\mathrm{c} = 0.23\,\mathrm{Torr\,cm}$$

$$j/p^2 = 450\,\mu\mathrm{A\,Torr^{-2}\,cm^{-2}}$$